UNIVERSITY OF INSUBRIA

VARESE

DEPARTMENT OF SURGICAL AND MORPHOLOGICAL SCIENCES

Adrenergic modulation of the intrinsic myogenic activity of peripheral diaphragmatic lymphatics

candidate:

Dott.ssa GRAZIELLA SANTORO

matr. 715838

PhD PROGRAM IN CLINICAL AND EXPERIMENTAL PHYSIOLOGY

XXVI CYCLE

SCHOOL OF BIOLOGICAL AND MEDICAL SCIENCES

Tutor: Prof.ssa DANIELA NEGRINI

Academic Year 2012-2013

A mia madre e a mio padre

che il mio grazie arrivi fin lassù…

Table of Contents

Summary

The diaphragmatic lymphatic system drains fluids and solutes from diaphragmatic interstitium and from the pleural and peritoneal cavities. Initial lymphatics, devoid of smooth muscle cells (SMCs) in their walls, join into long linear vessels or complex loops, formed at the confluence of linear vessels. Both linear vessels and loops, visible below the pleural and peritoneal mesothelia over the diaphragmatic dome, may be segmented in functional units, called lymphangions, separated by intraluminal valves, which ensure unidirectional lymph flow. Lymph progression within the diaphragmatic lymphatic vessels is due to an hydraulic pressure gradient of between adjacent lymphatic segments whose generation and maintenance depends upon a system of extrinsic and intrinsic pumps. Extrinsic pumping is mainly due to the movement of the surrounding tissues which causes the contraction/expansion of the vessel, while the intrinsic pumping mechanism is due to the rhythmic contraction of the smooth muscle cells surrounding the wall of the lymphangions. Extrinsic pumping prevails in lymphatics of the medial diaphragm, while lymphatic loops located at the extreme diaphragmatic periphery do require an intrinsic pumping mechanism to propel lymph centripetally. Lymph propulsion within the most peripheral diaphragmatic lymphatics depends upon tissue displacements and contraction of smooth muscle cells that surround the collecting lymphatics. The aim of the present work was to investigate, in actively contracting sites of peripheral diaphragmatic lymphatic vessels, the contribution of single strokes and valves opening/closing dynamics to lymph propulsion, and to analyze how this phenomenon is modulated by epinephrine.

Anaesthetized rats received an intraperitoneal injection of a mixture of FITC-conjugated dextrans and TRITC-labeled microspheres (0.1-1 μm diameter). After passive lymphatic

vessels loading, microspheres movement were video recorded *ex-vivo* in excised pieces of diaphragm, kept superfused with warmed oxygenated Tyrode's solution in a flow chamber on the stage of an upright microscope. Instantaneous and mean microsphere velocities were derived from microsphere trajectories along with vessel diameter changes due to spontaneous active strokes.

Data obtained show that active strokes exert a distance-dependent effect on microspheres progression from the contracting site. Their velocity profile results parabolic with a peak velocity of about 96 µm/sec. In the presence of intraluminal valves, microspheres show an oscillatory trajectory on the proximal side and monotonic outward directed flow on the distal side of the valve. Epinephrine administration has opposite effects in linear vessels and lymphatic loops: in particular, epinephrine determines an increase in contraction frequency of about 3 bpm and a greater distance traveled by microspheres in *loops* and an impairment of spontaneous activity in *linear* vessels.

1. Introduction

1. Introduction

1.1 The Lymphatic System

The anatomy of the lymphatic system was characterized by the early 19th century but already in 460-360 BC, Hippocrates described "white blood in nodes" in one of his medical texts, *On the Glands*, and Aristotle noted fibers containing colorless fluid located between blood vessels and nerves. Various aspects of lymph, lymphatic drainage and lymphatic anatomy have received attention in the 17th and 18th centuries. The lymphatic system was rediscovered in 1627 by an Italian anatomist, Gaspare Aselli as the "*venae albae et lacteae* (milk veins)", from the dog diaphragm (Asellius, 1627), and Swammerdam in the mid-1600s revealed valves in the collecting lymphatic vessels using wax injections. The nature and function of the lymphatic system were correctly described by William Hunter who proposed that the lymphatics are not continuations from arteries but are "a particular system of vessels by themselves" and that the lymph is formed by the absorption of fluid from the tissues into peripheral lymphatics (Hunter, 1762).

The lymphatic system develops in parallel, but secondarily to, the blood vascular system through the *lymphangiogenesis.* In the 20th century, researchers proposed two theories on the histogenetic origin of the lymphatic system: the "centrifugal model" and the "centripetal model". The first theory suggested that the lymphatic system is derived from the blood vascular system, in contrast, the other theory argued that the lymphatic endothelial cells are independently differentiated from lymphangioblasts derived from mesenchymal cells and that the primitive lymphatics are formed by these lymphatic stem cells first and later they connect to the embryonic vein. In 1902, has been demonstrated that the lymphatic system is derived from the early embryonic vein (Sabin, 1902, 1904). In birds and most mammal, lymphangiogenesis begins with the

formation of primitive lymph sacs as the result of the fusion of lymphatic capillaries. In humans, the first lymph sacs have been found nearly one month after the development of the first blood vessels (Van der Putte, 1975). In mice, the lymphangiogenesis starts after the cardiovascular system is functional (Oliver and Detmar, 2002).

For a long time the lymphatic system has been considered secondary to the other circulatory system, the blood vascular system, therefore modern molecular, cellular and genetic approaches have allowed to discover the real value of the lymphatic system. The lymphatic system operates in conjunction with the circulatory system. The blood vascular system is a circular system in which blood leaves the heart and returns to the same organ. In contrast, the lymphatic system is a blunt-ended linear system. As blood travels through the capillaries, fluid, proteins and cells enter the interstitial space according to a combined hydrostatic and osmotic pressure gradient. Most of this fluid is reabsorbed into the post-capillary venules, the excess enters the initial lymphatic capillary vessels, permeable to macromolecules, which originate in the interstitial spaces of tissue and organs. The fluid is then transported to thicker and larger collecting lymphatics and it eventually returns to the blood circulation through the thoracic duct that joins to the subclavian veins (Figure 1.1, Swartz, 2001, Choi et al., 2012).

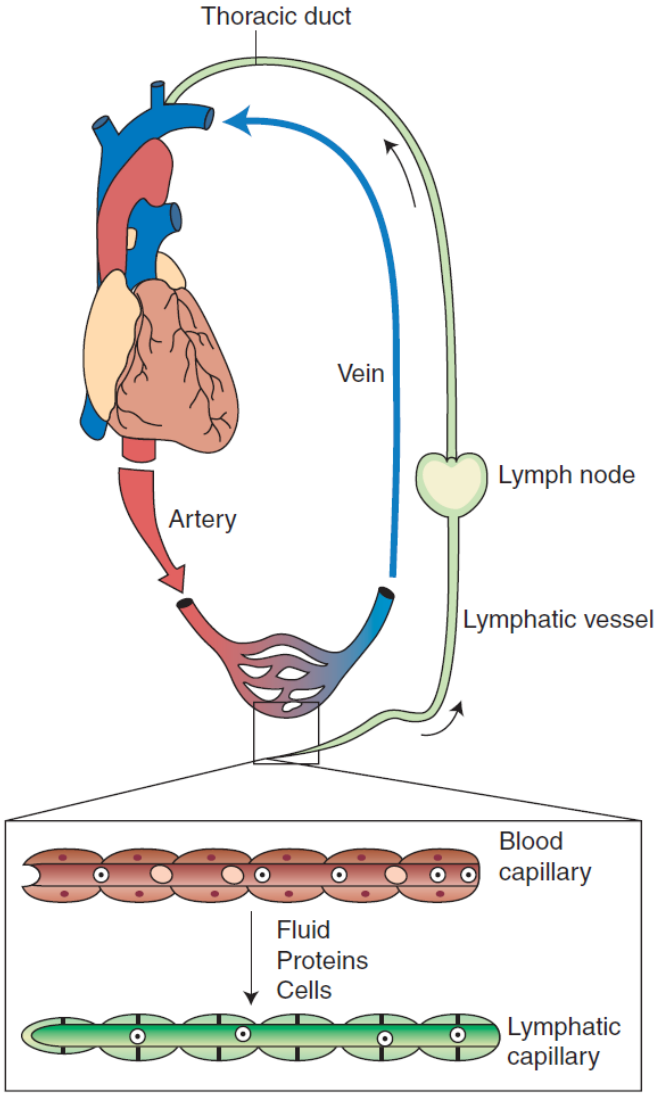

Figure 1.1 Macroscopic view of the blood versus lymphatic system. The blood vascular system is a circular and closed system in which the blood leaves from and returns to the heart; in comparison, the lymphatic system is a linear system in which the lymphatic capillaries drain the lymph and transport it back to the blood vascular system (Choi et al., 2012).

1.2 Anatomy of the Lymphatic System

The lymphatic system is present in most organs with the exception of the central nervous system, meninges, retina, internal ear, liver lobule, spleen pulp, kidney parenchyma, bone and avascular tissues, such as cartilage, nails and cuticle (Grey, 1918). It carries a transparent fluid called *lymph*, the vasculature is blind ending, small capillaries funnel first into pre-collecting and larger collecting vessels and then into the thoracic duct or the right lymphatic trunk, which drains lymph into the subclavian veins (Figure 1.2). The structure of the compartments reflects the dual role in lymph transport and in fluid absorption (Schulte-Merker et al, 2011).

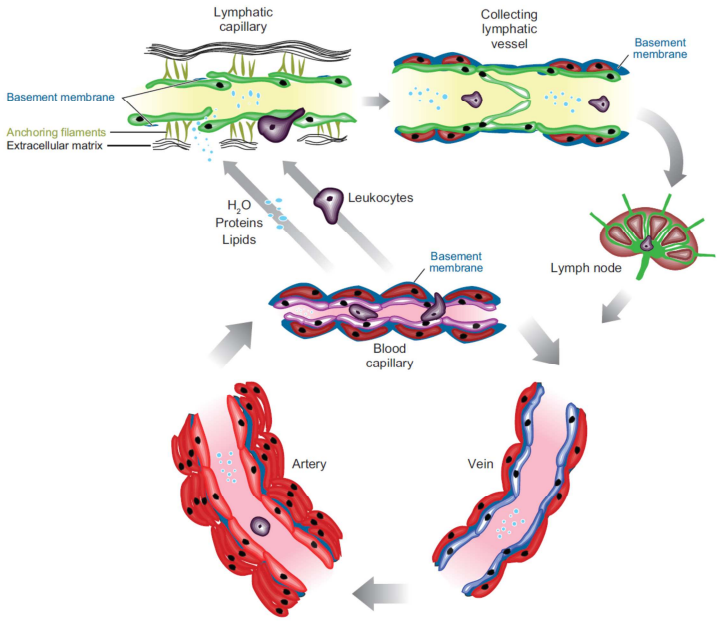

Figure 1.2. Structure of the lymphatic vessels. The lymphatic capillaries lack vascular mural cells and have no or only an incomplete basement membrane. The endothelial cells lack tight junctions, partly overlap, forming valve-like openings. Anchoring filaments connect lymphatic capillary endothelial cells to the extracellular matrix. The lymph is drained at the capillaries level and then propelled to pre-collecting and collecting lymphatic vessels that have a basement membrane, are surrounded by vascular smooth muscle cells with intrinsic contractility and contain valves. Finally, the lymph is filtered through lymph nodes. In contrast, the endothelial cells of blood vessels form tight and adherence junctions, have a basement membrane, and are surrounded by perycites/smooth muscle cells (Karpanen and Alitalo, 2008).

1.2.1 Initial lymphatics

Initial lymphatics (also called terminal lymphatics or lymphatic capillaries) have a diameter of about 10-60 μm and their wall has a thickness less than from 5 μm. The endothelial cells of lymphatic capillaries have a unique junctional organization (Baluk et al., 2007; Dejana et al., 2009) and are connected by discontinuous buttonlike junctions (Figure 1.3). Lymphatic capillaries are lined with a single layer of partly overlapping lymphatic endothelial cells (LECs) forming valve-like openings, called "flap valves", which allow easy access for fluid, macromolecules and cells into the vessel lumen (Trzewik et al., 2001; Galie and Spilker, 2009). These *primary valves* only permit unidirectional lymph entry into the lymphatic vessel lumen. The capillaries lack vascular mural cells and they have an incomplete or absent basement membrane, with the exception of lymphatic capillaries in the bat's wings (Hogan-Unthank, 1986). Anchoring filaments made of collagen VII (Leak and Burke, 1968), connect lymphatic capillary endothelial cells to the surrounding extracellular matrix (ECM) (Burgeson et al., 1990; Chen et al., 1997; Rousselle et al:, 1997) and keep them from completely collapsing when interstitial fluid pressure increases. These features make the initial lymphatics highly permeable to large macromolecules, migrating cells, and pathogens.

1.2.2 Pre-collecting lymphatics

The pre-collecting lymphatics connect the capillaries to the collecting vessels, they have indeed both lymphatic capillary (LECs) and collecting lymphatic vessel (valves) characteristics. They have a basement membrane, are surrounded by vascular smooth muscle cells (SMCs) in their walls, and are capable of performing spontaneous contractions. The pre-collecting vessels contain bicuspid one-way valves, irregularly

distributed that may comprise a single leaflet, to prevent the lymph backflow. The valve regions are devoid of SMCs (Sacchi et al., 1997).

1.2.3 Collecting lymphatics

The collecting lymphatics can be classified as *afferent* or *efferent* (*prenodal* or *postnodal*) depending on whether they carry lymph to or from the nodes. They are approximately 50-200 μm in diameter. The larger collecting lymphatics are covered with a continuous basement membrane and smooth muscle cells. Lymphatic muscle cells are found at the level of collecting vessels in most tissues and animals (Gnepp, 1984; Casley-Smith, 1968) with the exception of the bat wing (Webb, 1944) where they are found in the initial lymphatics. Endothelial cells are elongated and connected by continuous zipperlike junctions (Figure 1.3) which, together with the basement membrane, prevent lymph leakage during the transport. They contain the *secondary valve system* that allows lymph propulsion and prevents retrograde flow (Takada, 1971). Segments of collecting lymphatics between valves are called lymphangions: a contractile compartment that propels lymph into the next compartment (Granger et al., 1984).

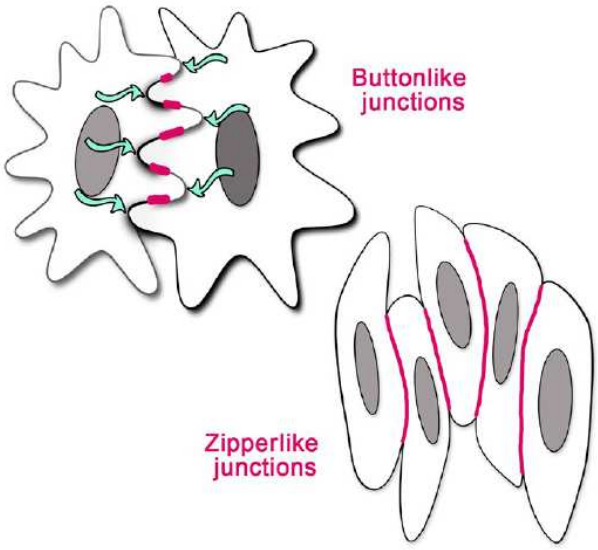

Figura 1.3. Junctional organization of lymphatic endothelial cells in lymphatic capillaries and collecting vessels. Both button and zipperlike junctions present adherens and tight juntions-associated proteins (e.g., VE-cadherin, zonula occludens-1, occludin, and claudin-5, with different organization (Shulte-Merker et al., 2011).

1.2.4 Lymphoid organs

Lymphoid organs are classified in primary and secondary. The primary (thymus and bone marrow) are responsible for the production and maturation of lymphocytes; the secondary organs (spleen, Peyer's patches, appendix, tonsils and nodes) are responsible also for initiation of an immune response. The collecting vessels pass through capsular lymph nodes that are organized in clusters throughout the lymphatic system. Lymph nodes are interspaced in the collecting vessels and act as filters for the lymph as it passes through. Lymph nodes are 1-10 mm in diameter and there are hundreds of lymph nodes in the adult human body. The exterior walls are covered with lymphatic smooth muscle which causes contraction even if at a low frequency. The outer surface is covered by sinus-lining cells that create an impermeable membrane (Roozendaal R. et al., 2008), thus large molecules cannot penetrate this layer and this prevents pathogens from reaching the bloodstream.

1.2.5 The secondary valve system

The system of intraluminal or secondary valves, which is present in the collecting lymphatics, prevents reflow along the lymphatic vessels. The segment delimited by two consecutive intraluminal valves, the lymphangion, is the "functional unit" of the lymphatic vascular system (Granger, 1984). Each lymphangion consists of a contractile compartment with an inlet and an outlet valve. Chains of lymphangions, as seen along the collecting lymphatics, serve as entry-valves and exit-valves from one compartment to the next (Schmid-Schonbein, 2003). The valves contain two semilunar leaflets, which are covered on both sides by a specialized endothelium anchored to the extracellular matrix core (Lauweryns and Boussauw, 1973). The valve leaflets, long about twice the length of the lymph cross-sectional dimension, form a funnel inside the lymphatic channels (Mazzoni et al., 1987). Each leaflet is attached at opposite sides, to the lymphatic wall, and toward their downstream end they fuse together to form a buttress. The buttress is attached to the wall so that its free ends form the opening for the passage of lymph fluid. The two buttresses prevent inversion of the leaflets (Figure 1.4).

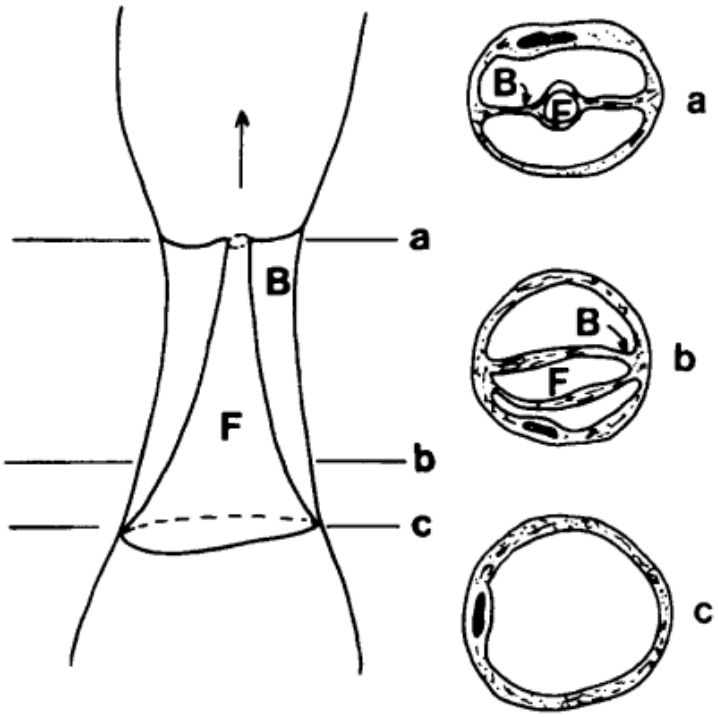

Figura 1.4. Funnel arrangement of lymphatic valves. Funnel (**F**) consists of a thin connective tissue sheet covered by lymphatic endothelium. Inversion of funnel is prevented by attachment to lymphatic wall via two buttresses. Arrow indicates flow direction. **a**, **b**, and **c** drawings of cross sections taken at the indicated level in the left panel drawing (Swartz, 2001).

The mechanism of leaflet opening and closure can be represented by considering the fluid pressure at different points around the leaflets: P_1 in front of the valve, P_2 downstream and P_3 in the sinuses (Figure 1.5). In the funnel region the lymph fluid motion is accompanied by viscous dissipation, so that during a downstream motion $P_1 > P_2$. When the sinuses are closed $P_2 = P_3$, little or no motion occurs. Subsequently, the pressure drop across the leaflets, $P_1 - P_3$ is positive, and thus the valve leaflets are pushed open. The flow stops when $P_1 = P_2 = P_3$ or when $P_3 > P_2 > P_1$ and the trans leaflet pressure vanishes.

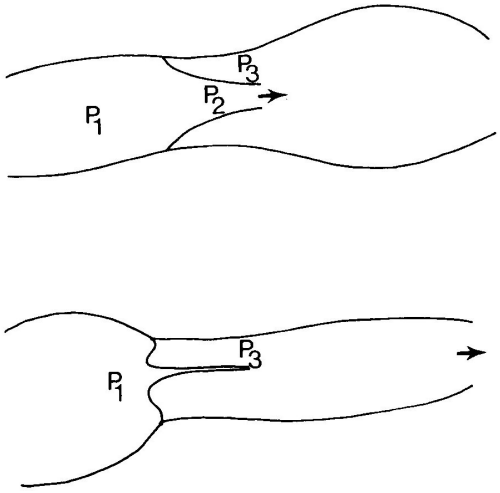

Figure 1.5. Lymphatic pressure in vicinity of valve. P_1, upstream pressure, P_2, downstream pressure, P_3, abluminal pressure in outer pocket of valve leaflet. $P_2 - P_3$, is trans leaflet pressure drop. $P_1 > P_2 > P_3$ in condition of flow; during closure $P_1 = P_2$ so that $P_2 - P_3 < 0$.

Most lymphatic secondary valves are of the bicuspid type (Albertine et al., 1987) but some have been found tricuspid, and occasionally even valves with a single leaflet (Gashev and Zawieja, 2001). Data about the size, the geometry and the number of valves are scarce, such as on the structure and operation of the secondary valves (Gashev and Zawieja, 2001), although valve size varies with the vessel calibre. Studies of the rat spinotrapezius muscle have shown that smooth muscle cells are absent from the valve leaflets (Mazzoni et al., 1987); the valve operation is determined by the pressure and viscous forces associated with the flow of the lymph. The vessel muscle tone influences the pressure gradient. A two-valves system is required to prevent backflow and to guarantee the unidirectional transport in lymphatics. Two neighbouring valves are never open at the same time (Ohhashi, 1980): one is open, while the other one is closed, so unidirectional transport is possible. The presence of the valves is essential for contraction because they allow a lymphangion to distend before emptying into the next segment: this results in a net pressure drop along the entire length of the vessel, and the flow of the lymph ceases when rhythmic contractions stops (Ohhashi, 1980). The opening and the closing of valves depend on periodic changes in fluid

pressure within collecting vessels. High lymph pressure upstream of a valve opens the valve and enables lymph flow, reverse flow pushes the leaflets against each other and closes the valve (Figure 1.6, Shulte-Merker et al., 2008).

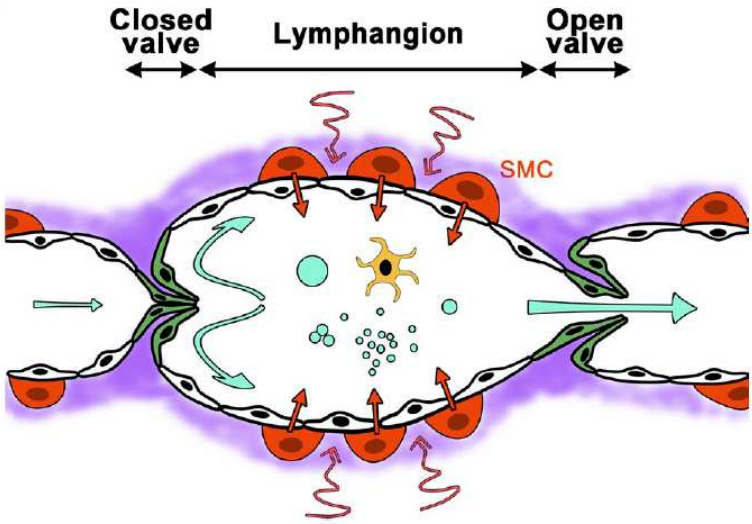

Figura 1.6. Lymphangion and lymphatic valve. High lymph pressure upstream of a valve opens the downstream valve and enables lymph flow, whereas reverse flow pushes the leaflets against each other and closes the upstream valve (Schulte-Merker et al., 2011).

1.3 Functions of the Lymphatic System

Lymphatic vessels are essential for transporting tissue fluid, extravasated plasma proteins and cells back to the blood circulation, thus contribute to the maintenance of fluid homeostasis. The lymphatic system not only controls the tissue fluid homeostasis, but also maintains plasma volume constant, contributing to the regulation of arterial pressure and cardiovascular function, it contributes to immune response through lymph nodes promoting the return of leukocytes and cells, including tumoral cells, to the blood stream and it serves as a reservoir for extracellular fluid (Negrini, 2011). The lymphatic system also serves as a conduit for trafficking of lymphocytes and antigen-presenting cells from the interstitium to be displayed for B and T cells in the lymph nodes. The activated immune response cells proliferate in the lymph nodes and produce antibodies. Cells and antibodies are delivered into the circulation via the lymphatics (Jeltsch et al., 2003).

1.4 Lymph formation

The net flow rate in the lymphatic vessels is due to lymph formation and lymph propulsion that are determined by multiple factors, passive and active. The first describes the fluid transport from the interstitium into the initial lymphatics, while the second refers to the forces that drive lymph from the capillaries into the larger collecting vessels and eventually back to the blood. The lymph formation depends by local forces such as interstitial fluid pressure and extracellular matrix strain (Swartz, 2001); on the other hand, lymph propulsion is also driven by extrinsic forces exerted by respiratory activity and/or blood pressure swings, and it can be modulated by the influence of neurotransmitters and hormones. Lymph enters through the openings in endothelial cells of the capillaries. These primary valves open when interstitial pressure increases above intraluminal pressure and this allows the fluid flow to enter initial lymphatics. When the pressure inside the vessels rises above interstitial pressure, the valves close (Figure 1.7). Lymph formation is organ dependent because of the different mechanical stresses that each tissue exerts upon lymphatic vessels in the various organs (Margaris and Black, 2012).

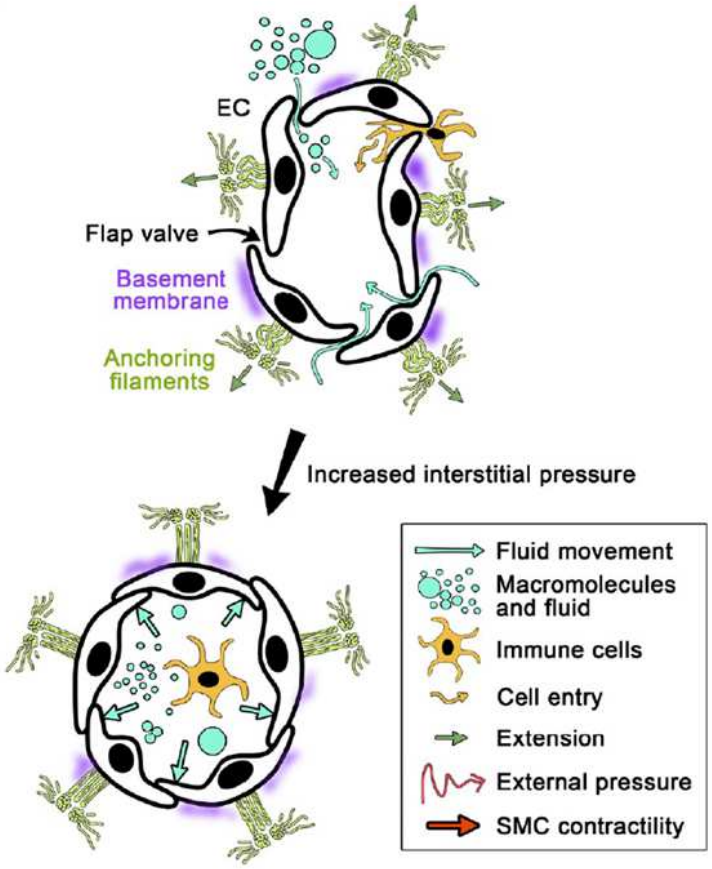

Figura 1.7. Mechanism of lymph formation in lymphatic capillaries. Interstitial components penetrate initial lymphatics via openings between endothelial cells. Anchoring filaments attach the endothelial cells to the extracellular matrix and prevent vessels from collapsing (Shulte-Merker et al., 2011).

1.4.1 Starling's Law

Lymph formation is driven by the combined hydrostatic and colloidosmotic pressure gradient and modulated by the permeability of the endothelial wall or conductance. The Starling's equation describes this kind of phenomenon:

$$J_v = L_p \cdot A_m \cdot [(P_{in} - P_l) - \sigma(\pi_{in} - \pi_l)] \quad \text{(Eq. 1.1)}$$

where J_v (nl/sec) is the lymph drainage rate, L_p is the hydraulic permeability to water of the endothelial barrier of initial lymphatics (cm/sec · cmH_2O), A_m is the endothelial exchange surface area (cm^2), P_l is the intraluminal lymphatic hydrostatic pressure (cmH_2O), P_{in} is the interstitial hydrostatic pressure (cmH_2O), π_l is the lymph oncotic pressure (cmH_2O) and π_{in} is the interstitial oncotic pressure (cmH_2O), σ is the capillary oncotic reflection coefficient ($\sigma = 0$ means completely permeable without protein reflection: $\sigma = 1$ means completely impermeable with 100% protein reflection).

The Starling' Law can be summarized as:

$$J_v = L_p \cdot A_m \cdot [\Delta P - \sigma \cdot \Delta\pi] \quad \text{(Eq. 1.2)}$$

where ΔP and $\Delta\pi$ are the local hydrostatic and oncotic pressure differences across the lymphatic capillary wall. For the lymphatics, the product $\sigma \cdot \Delta\pi$ is typically considered negligible with respect to ΔP because their reflection coefficient approaches a value of zero, that is, significantly lower than that of blood capillaries (Schmid, 1990; Leak et al.,1966; Hammersen F. and Hammersen E, 1985; Castenholz, 1984). L_p is not constant for lymphatic capillaries and depends on the state of stress of the tissue (Figure 1.8).

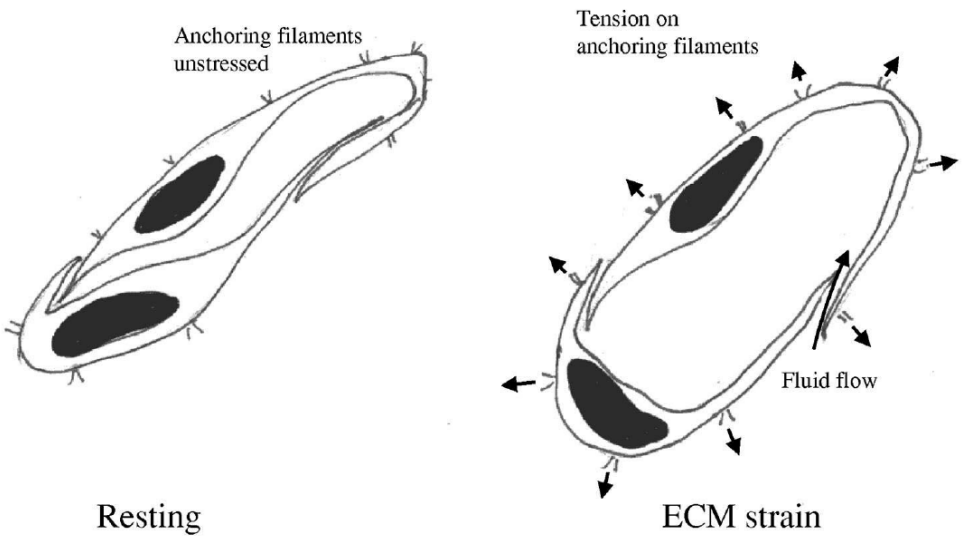

Figura 1.8. The "tissue pump" for lymph formation. The stress within the interstitium creates radial tension on anchoring filaments. The luminal volume of lymphatic capillaries increases and this creates a transitory pressure gradient favouring the flux of interstitial fuid into the lymphatics (Swartz, 2001).

Thus, in initial lymphatics $\sigma_d = 0$ and $\pi_{in} = \pi_l$:

$$J_l = L_p \cdot A_m \cdot \Delta P_{lymph} = L_p \cdot A_m \cdot (P_{in} - P_l) \qquad \text{(Eq. 1.4)}$$

If P_{in} is higher than P_l, the ΔP_{lymph}, gradient is positive and the fluid flux goes from interstitial space into the initial lymphatic lumen, opening the primary valves. A negative ΔP_{lymph} gradient due to P_l higher than $P_{in,}$ might allow the lymph backflow in the interstitial space but this event is prevented by flap-valve closure.

1.5 Pathologies of the Lymphatic System

Defects of the lymphatic vasculature are implicated in a variety of human pathologies. The lymphatic vessels have an important role in tumor metastasis and inflammation (Sleeman et al., 2009; Tammela and Alitalo, 2010). The lymphatics serve as a primary route for the dissemination of many solid tumors such as breast, colon, lung, and prostate tumors, to the regional lymph nodes and possibly via the thoracic duct and the blood circulation, to distant organs. Tumor cells more easily penetrate lymphatic vessels than blood vessels, because of the looser junctions between ECs and basement membrane (Alitalo and Carmeliet, 2002). On the other hand, tumor cell metastasis to lymph nodes represent an optimum criterion for evaluating the prognosis of patients and for choosing a suitable therapy.

Lymphedema is due to accumulation of interstitial fluids caused by lymphatic dysplasia, malformation, misconnection, and obstruction and/or absence of functional lymphatic valves. Complications of lymphedema include progressive dermal fibrosis, accumulation of adipose and connective tissue, decreased immune defense (Rockson, 2001). Lymphedema is classified as primary (genetic) or secondary (acquired) (Figure 1.9). This last pathology is consequence of a disease, trauma, surgery, or radiotherapy.

1.5.1 Primary Lymphedema

Primary lymphedema can be divided into three groups depending on the age of onset: *congenital* lymphedema (at birth), lymphedema *praecox* (early onset), and lymphedema *tarda* (late onset) (Allen, 1934). Congenital lymphedema manifests more often in females than males, in lower extremities, and in a single rather than both legs. A subgroup of congenital lymphedema, the *Milroy disease* (Milroy, 1892, 1928) is

characterized by absence of the lymphatic vessels or, if they are present, they are extremely hypoplastic in the affected areas, but not in the unaffected ones (Brice et al., 2005). Lymphedema praecox, often called *Meige's disease,* is commonly detected around the puberty. Females are affected four times more often than males. The patients display dysplastic, smaller, and fewer lymphatic vessels compared to healthy individuals (Finegold et al., 2001).

Lymphedema-distichiasis syndrome, a subset of lymphedema praecox, is characterized by edema of the limbs and it is associated with a variety of congenital abnormalities. The third type of primary lymphedema is called *lymphedema tarda,* in effect, the symptoms manifest only at a late stage of life, usually after age 35. This form displays a tortuous, hyperplastic pattern of lymphatic vessels characterized by an increase in diameter and number and their patients often lack functional lymph valves (Choi et al., 2012).

1.5.2 Secondary Lymphedema

Postsurgical edema, especially after mastectomy, represents the primary form of lymphedema in industrialized countries. It may develop in upper or lower extremities or in external genitals because of invasive surgery, trauma, radiation. The most common causes of secondary lymphedema, especially in Africa and Asia, is *filariasis*, a direct infection of lymphatic vessels by mosquito-borne parasitic nematodes like *Wuchereria bancrofti*, *Brugia malayi*, or *Brugia timori*. These parasites cause a dilatation of lymphatic vessels and eventually a complete and permanent disruption of lymphatic transport, which leads to a predisposition to long-term recurrent bacterial infections and a condition known as elephantiasis (Dreyer et al., 2000).

Lymphedema presents severe social, economic, and psychological burdens to patients and their families, and, no cures are available for this disease.

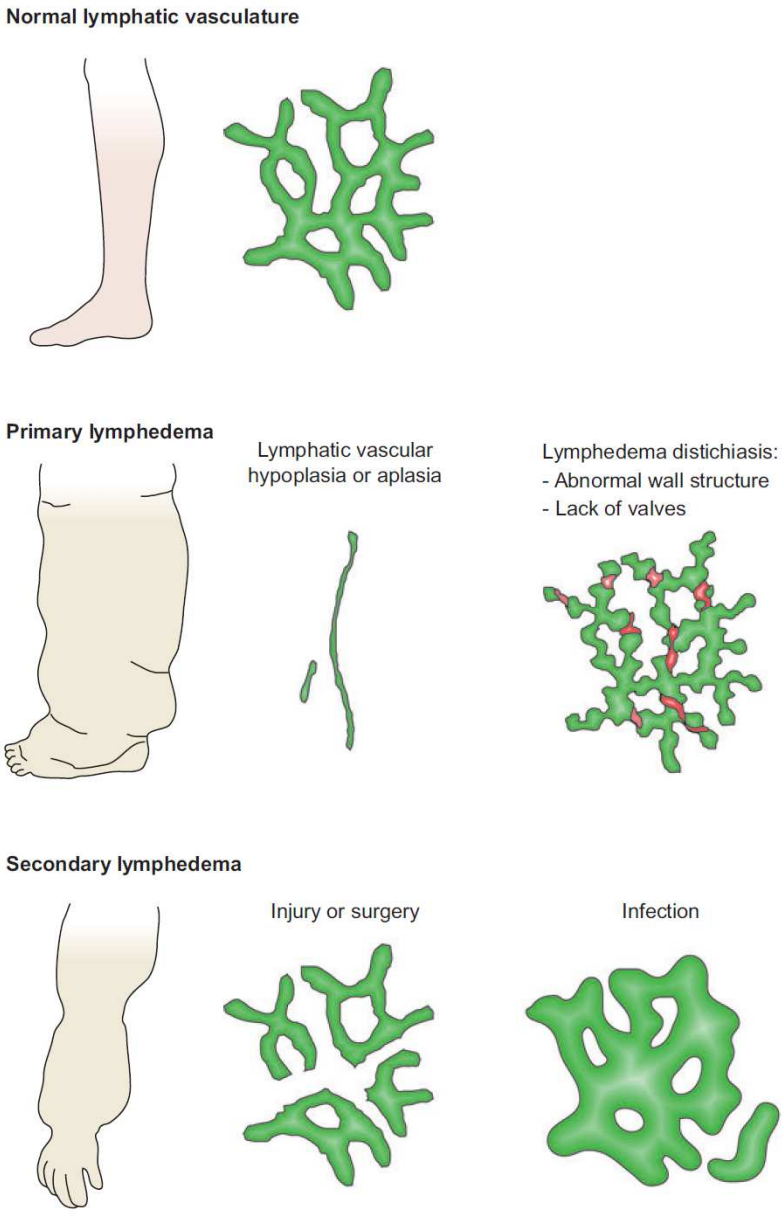

Figura 1.9. Lymphedema. Hereditary lymphedema can be caused by total absence or severe reduction of lymphatic vessels or by abnormal morphology. Secondary lymphedema is due to disruption or trauma of lymphatic vesselsby injury, surgery or infection (Karpanen and Alitalo, 2008).

1.6 The Diaphragm

The diaphragm is a dome-shaped fibro-muscular lamina that separates the thoracic cavity from the abdominal cavity. The diaphragm is controlled by somatic and autonomous nerve fibers, and it is exclusively innervated by the phrenic nerve. The central portion of the diaphragm is tendineous, and it is surrounded by a ring of radially oriented striated muscle fibers (Figure 1.10). This muscle fibers are inserted on the sternum, on the ribs and on the lumbar vertebrae. The diaphragm plays a very important role in the ventilation process, it is responsible for most of the work of breathing of a normal person. The phrenic nerve controls the movements of the diaphragm that regulate the breathing. The lungs are enclosed in a kind of cage in which the ribs form the sides and the diaphragm forms the floor. During inspiration, the diaphragm is moved down (Boriek et al., 2005) and becomes flat, the chest cavity becomes larger and the intercostal muscles expand the ribs. The diaphragm is covered by one layer of peritoneum and by the inferior surface of the parietal pleura, thus when it contracts it pulls the pleura with it. The pleural pressure decreases and causes the alveolar pressure to drop. This generates a pressure gradient which lets air to flows into the lungs. During expiration, the diaphragm passively relaxes and returns to its equilibrium position.

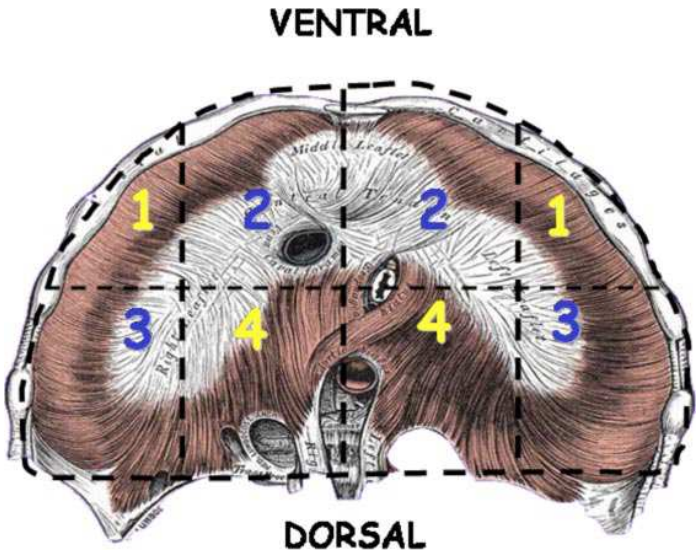

Figure 1.10. Schematic front of the diaphragm. The shaded areas correspond to the medial tendineous tissue (light shading) and the peripheral muscular (dark shading) portions. *Region 1*, ventrolateral area corresponding to ventral peripheral muscular portion; *region 2*, medial ventral portion corresponding to ventral tendineous area; *region 3*, dorsolateral muscular region; *region 4*, dorsomedial tendineous region (Grimaldi et al., 2006).

1.7 The diaphragmatic Lymphatic System

The diaphragmatic lymphatic system has been an object of different research for many years. Recklinghausen in 1863 suggested the presence of small openings, or stomata, that connect the lymphatic lumen and the peritoneal cavity. In 1903, MacCallum found that tracers injected into the peritoneal cavity migrated into the diaphragmatic peritoneal vessels via lacunae, ample lymphatic spaces. Stomata (figure 1.11) and lacunae (figure 1.12) are, in fact, representative structures of the pleural and peritoneal lymphatic system of the diaphragm.

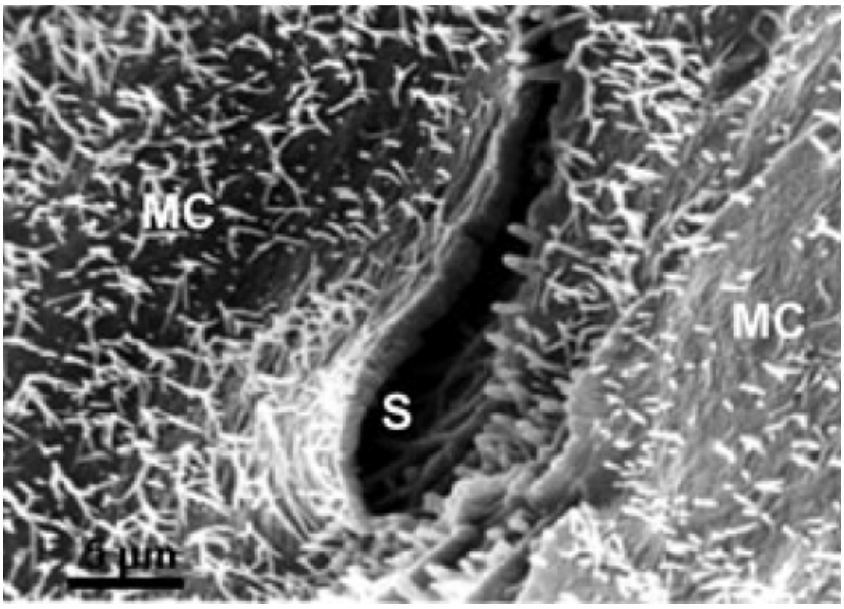

Figura 1.11. Lymphatic stoma on the tendinous pleural surface of the rat diaphragm. The stoma (S) opens at the confluence between adiacent mesothelial cells (MC) characterized by a mesh of microvilli protruding from the cell surface (Negrini et al., 1991).

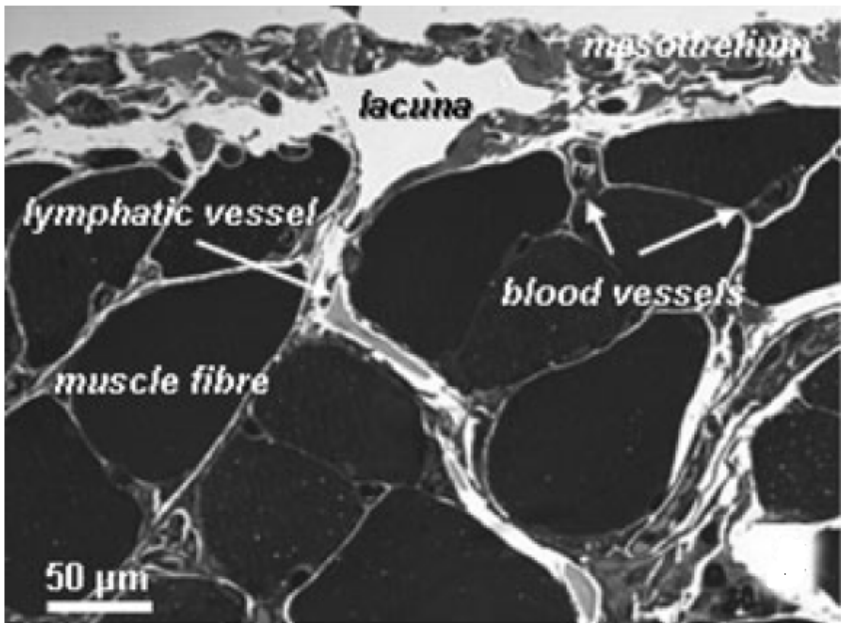

Figura 1.12. Diaphragmatic lymphatic network. Lymphatic submesothelial lacunae located within the interstitial space under the mesothelial layer are in continuity with the lymphatic vessels (arrow) which run perpendicular to the lacunae and through the skeletal muscle fibers (Negrini et al, 1992).

The submesothelial lacunae show a discontinuous endothelium (different components in figure 1.13) and are characterized, on their mesothelial side, by several discontinuities,

the stomata (Negrini et al., 1991; Ohtani et al., 1993; Wang, 1975). The lymphatic lacunae receive the fluid drained from pleural and peritoneal cavities by the stomata, present between the mesothelial cells. Stomata are open to the pleural and peritoneal cavites on the roof of lacunae, formed at the confluence between mesothelial cells, that allow non-specific passage of fluid and particulate matter; the openings might act as a lymphatic sieve (Shinohara, 1997). In rabbits, stomata are abundant on the central tendineous part and sparse on the muscular region (Allen, 1967; Negrini et al., 1991); in mice (Tsilibary and Wissig, 1977; Leak and Rahil, 1978) and in rat (Abu-Hijleh et al., 1994) they occur only in the diaphragmatic muscular portion; in the golden hamster they are present in both parts of the diaphragm (Fukuo et al., 1990). There is a correlation between the distribution of mesothelial stomata and submesothelial lymphatic lacunae (Negrini et al., 1991). In the rabbit, the density of lymphatic lacunae and consequently the mesothelial stomata density are higher on the peritoneal than on the pleural side (Negrini et al., 1991).

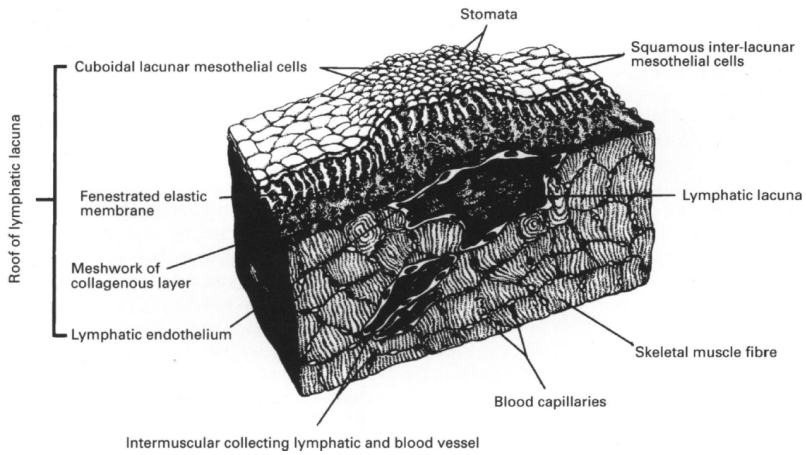

Figure 1.13. Three-dimensional diagram of the rat diaphragm. Different component of the lymphatic lacunar roof. The peritoneal surface is uppermost (Abu-Hijleh et al., 1994).

Thus, the diaphragmatic lymphatic network, by draining the pleural liquid, helps to maintain the volume of the pleural cavity to the minimum value (Negrini et al., 1985). The initial lymphatic vessels are organized in planar submesothelial pleural and peritoneal lacunae and transverse lymphatic capillaries, which depart perpendicularly from the lacunae and empty in larger collecting lymphatics (Grimaldi et al., 2006; Negrini et al. 1992; Ohtani et al., 1992; Wang, 1975). The stomata diameter range is from less than 1 μm to 20-30 μm (Wang, 1975; Negrini et al., 1991) and thus solutes as large as cells can enter the deeper submesothelial lymphatic structures (Negrini et al., 1992, Grimaldi et al., 2006). On the contrary, adjacent mesothelial cells are connected through intercellular tight junctions and desmosomes (Mariassy and Wheeldon, 1983; Wang, 1998) that limit paracellular transport of large solutes to the submesothelial interstitium. Collagen bundles connect the outer surface of the vascular and lymphatic endothelium to the tissue and skeletal muscle fibers (Grimaldi et al., 2006).

Diaphragmatic lymphatic vessels, on the pleural side, are anatomically different for arrangement and for distribution from peritoneal lymphatics. The diaphragmatic peritoneal lymphatic vessels have extremely flat lumina, they are usually from several to 100 μm in width. The lymphatic vessels appear serrated as a result of the extension of numerous short branches to adjacent vessels (Fig. 1.15A, insert). Peritoneal submesothelial vessels are organized in distinct areas, they extend radially and parallel to one another from the central tendon border to the thoracic wall. In contrast, the pleural lymphatic vessels are tubular and they have a diameter range from a few to several hundred micrometers (Fig. 1.15B). Pleural diaphragmatic limphatic vessels are organized into planar submesothelial linear vessels or complex loops, formed at the confluence of long linear vessels (Figure 1.14) (Negrini and Del Fabbro, 1999; Negrini et al., 2004).

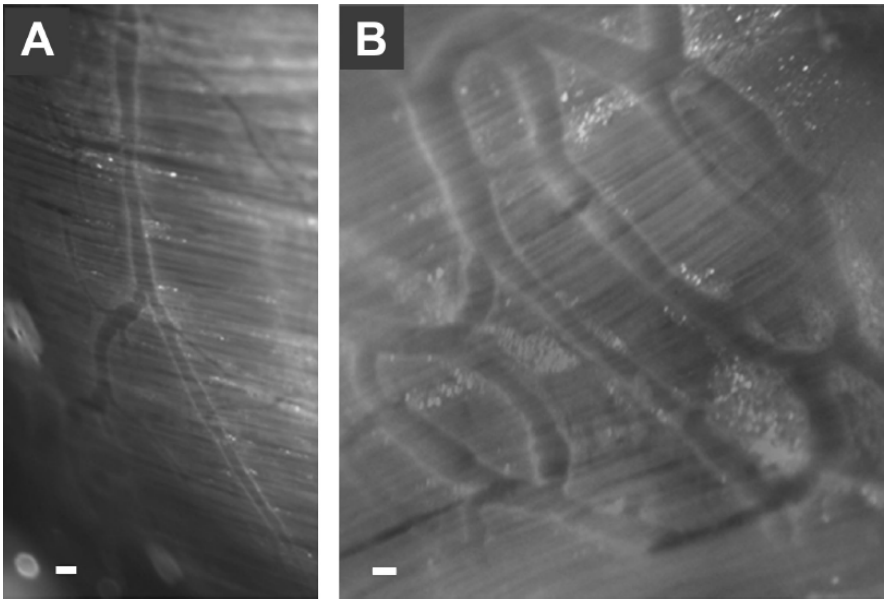

Figure 1.14. White-light epi-illuminated stereomicroscope images of the medial pleural diaphragmatic surface: (**A**) a linear lymphatic vessel (Scale bar:100 μm); (**B**) a lymphatic loop (Scale bar: 200 μm) (Moriondo et al., 2008).

Diameters of the two populations of lymphatic vessels are greater in linear (103.4 ± 8.5 um) than in loop (54.6 ± 3.3 um) (Moriondo et al., 2008). The loops are mainly located in the peripheral ventrolateral region of the diaphragm, whereas the linear vessels are located in the medial area of the diaphragm. They are arranged in radial and reticular patterns. The radial arrangement was seen from the tendon–muscle border to the mid-muscle portion. These lymphatics connect with several short, transmuscular branches from the lymphatic vessels on the peritoneal side (Fig. 1.15B, asterisk and white arrows). As they approach the thoracic wall, lymphatic vessels extend transverse branches which traverse muscle fibers and interconnect with the adjacent lymphatics. The continuation of these traversing branches seems to form a lymphatic pathway that extends around the diaphragm along the thoracic wall and empty into the retrosternal lymphatic vessels (Fig. 1.15B, black arrows).

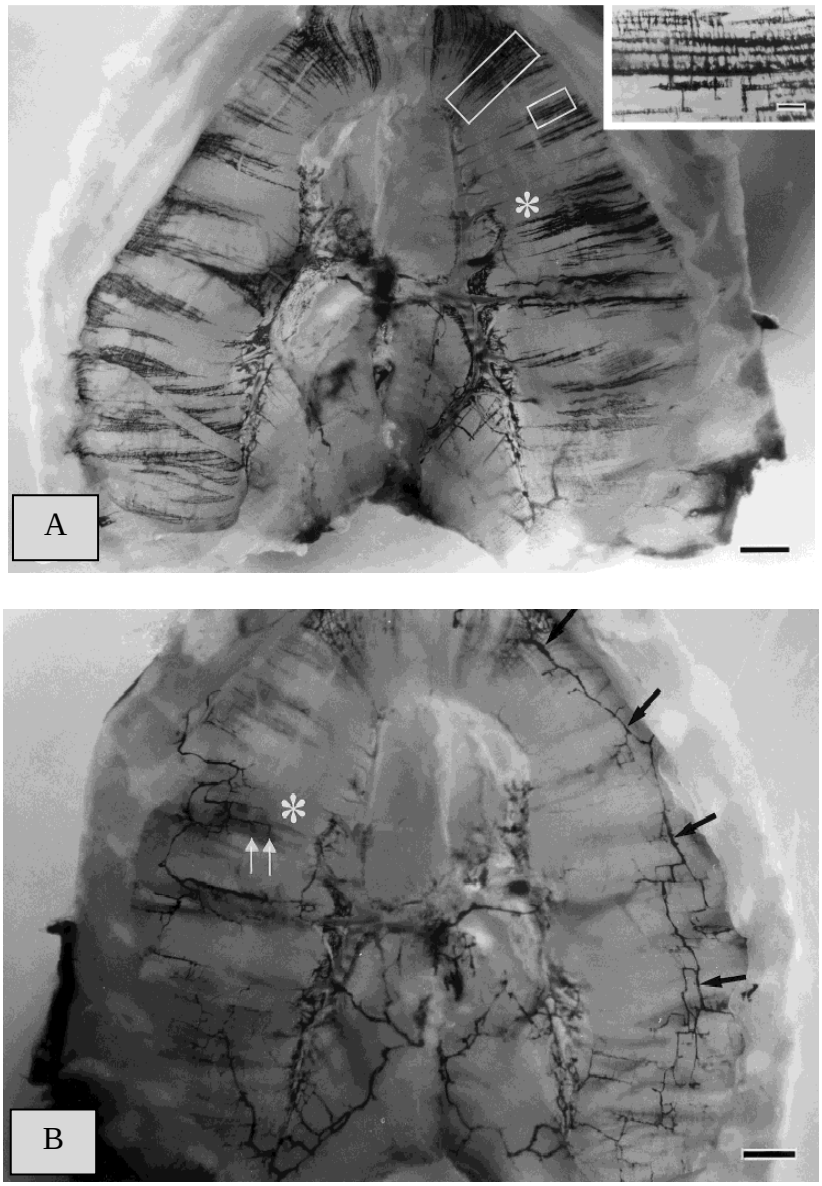

Figure 1.15. Diaphragmatic lymphatic system. Different diaphragmatic lymphatic vessels arrangement on both peritoneal (**A**) and pleural (**B**) side. Peritoneal vessels extend radially and parallel from the central tendon to the thoracic wall. The lymphatic vessels appear serrated as a result of the extension of numerous short branches to adjacent vessels (insert). Pleural lymphatics were arranged in radial and reticular patterns and they made contacts with several short, transmuscular branches from the lymphatic vessels on the peritoneal side (Scale bar: 1mm) (Shinohara, 1997).

The pleural submesothelial interstitial tissue is significantly thicker (~35 μm) respect to the peritoneal region (~20 μm). Also, the lacunae density is higher over the peritoneum compared to the pleural one (Grimaldi et al., 2006). Small numbers of lymphatic stomata on the pleural surface of the diaphragm together with morphological differences

might be related to different functional roles, in effect, although the mechanisms supporting lymph formation and propulsion from the cavities are the same, the amount of fluid removed from the peritoneal cavity is much larger than from the pleural side (Negrini et al., 1991,1992,1993,1994).

Fluid and solute flux between the pleural and peritoneal cavities might play an important role in pathological conditions associated with the development of ascites and in the processes of tumor dissemination (Grimaldi et al., 2006).

1.8 Lymphatic pumping and lymph propulsion

Lymph propulsion is generated by extrinsic and intrinsic mechanisms. The lymphatic system requires phasic and tonic lymphatic contractions to generate and regulate the flow of the lymph. The *passive* or *extrinsic* lymph pump is due to the influences of other forces and is predominant in the lymphatics of the heart, skeletal muscle, thorax, and the gut wall, while the intrinsic pumps are essential for lymph flow in most other lymphatic beds. Extrinsic forces include the influence of cardiac and arterial pulsation on neighbouring lymphatic vessels, the contraction of skeletal muscles adjacent to the vessels, central venous pressure fluctuations, gastrointestinal peristalsis and respiratory movements. These forces generate hydrostatic pressure gradients that allow the lymph propulsion. Extrinsic pumping prevails in lymphatics of the medial part of the muscular and tendineous diaphragm (Moriondo et al., 2005, Negrini et al., 2004), while lymphatic loops, located at the extreme diaphragmatic periphery, require an intrinsic pumping mechanism to propel lymph centripetally (Moriondo A. et al., 2013). A dense smooth muscle mesh surrounds actively pumping sites, whereas in not contracting tracts smooth muscle fibers were more sparsely organized.

The *active* or *intrinsic* pumping describes the lymph driving force generated by the active, rhythmical, and spontaneous contraction of lymphangions (Mislin, 1976). The contraction of smooth muscle cells present in wall of collecting vessels leads to a reduction of the lymphatic diameter, an increase in the local lymph pressure, closure of the upstream lymph valve, opening the downstream lymph valve, and ejection of some fraction of the lymph within that vessel. The contraction propagates along the lymphatic, producing a pulse in lymph flow. This is the primary mechanism by which lymph is propelled centrally. This activity persists in the presence of nerve inhibitors

(tetrodotoxin) and in absence of an intact endothelium (McHale and Roddie, 1980; Hanley et al., 1992). The contractions are the result of pacemaker cells located within the lymphatic wall, that depolarize and induce an action potential or group of action potentials. The depolarization produces an increase in intracellular calcium (Van Helden, 2000; Zawieja et al., 1999) which enters the cell through L-type Ca^{2+} channels, (McHale and Allen, 1983, Atchison et al., 1998) leading to contraction of the actin/myosin filaments within the muscle cells (Shirasawa and Benoit, 2003; McHale and Allen, 1983). The action potentials rapidly propagate through all the smooth muscle cells in a lymphangion to allow a synchronized contraction. The smooth muscle cells are, in fact, electrically coupled and act as a functional syncytium. The action potentials propagate through gap junctions which connect adjacent lymphatic smooth muscle cells; they have been detected in bovine mesenteric lymphatics (McHale and Meharg, 1992). The identity of pacemaker cells is not clear, but they are located within the muscle layer of the lymphatic wall.

The lymphatics act similar to the heart in generation of flow. The contractile cycle of these vessels can be divided into systole and diastole (Granger, 1979; Granger et al., 1977). The intrinsic lymph pump can be modulated via inotropic (changes in the contraction strength) and/or chronotropic (changes in the contraction frequency) fashion by physical factors and chemical agents (Von der Weid and Zawieja, 2004). Chemical mediators can modulate the lymphatic pumping acting in different ways. The circulating and interstitial modulators are factors present in the lymph or released from the blood stream and cells in the interstitial fluid. In effect, large lymphatic vessels are supplied with blood through small vessels similar to *vasa vasorum* (or *vasa lymphorum*) which can carry mediators that act on lymphatic vessels. The lymphatic vessels release various chemical mediators that can act in an autocrine or paracrine manner (e.g. nitric oxide

released by the lymphatic endothelium) (von der Weid et al.,1996). There are also modulators released upon stimulation from nerve endings that surround the vessels (McHale et al., 1980; Allen et al.,1983; McHale et al., 1991) (Figure 1.16).

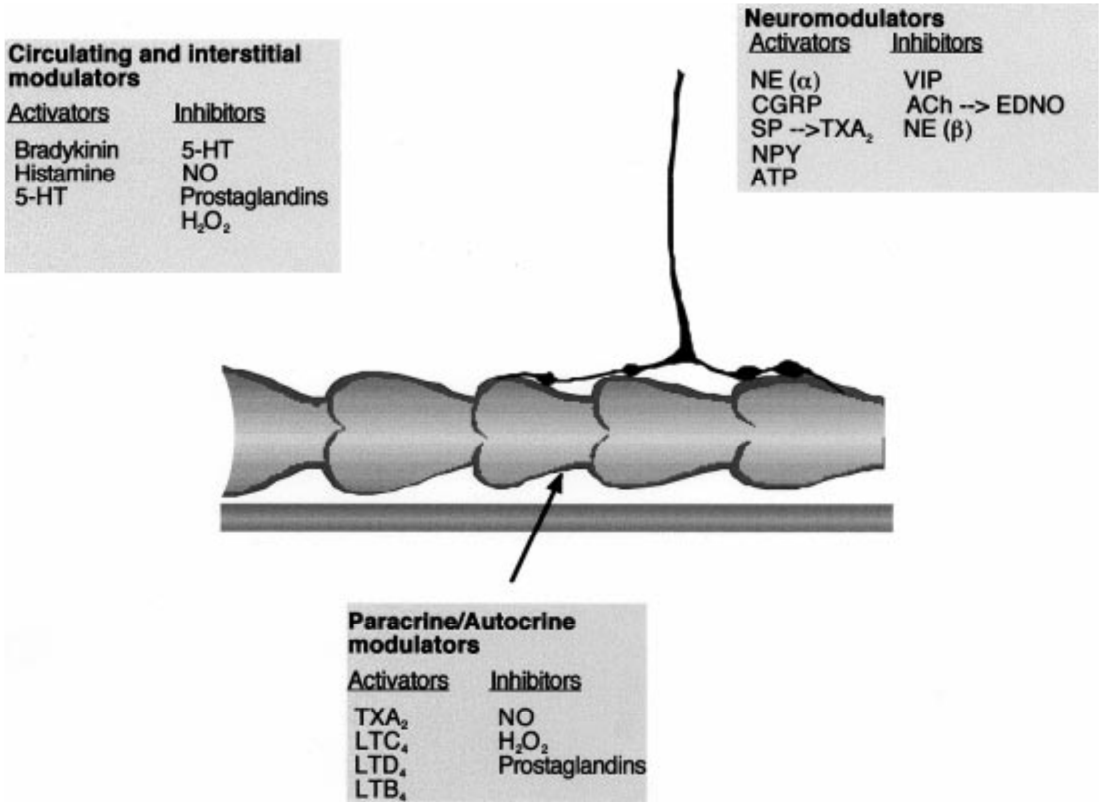

Figure 1.16. Different ways of modulation of spontaneous lymphatic constriction by chemical mediators (von der Weid, 2011).

The physical factors such as transmural pressure, luminal flow and shear stress, can modulate lymphatic tone and function (Zawieja, 2009); increasing in vessel wall stretch induces enhancements both in lymphatic contraction frequency and in contraction strength. Humoral factors such as α-adrenergic and β-adrenergic agonists, prostaglandins, bradykinin, substance P and others can modulate both lymphatic vessels' tone as well as alter the active pumping activity.

1.9 Effect of inflammatory mediator on electrical pacemaker potential

The inflammatory mediators affect the pacemaker potential mechanism that initiates intrinsic contractions. The pacemaker activity has been described as spontaneous transient depolarizations. In the regulation of smooth muscle tone is involved the endothelium of lymphatic vessel. In effect, it modulates the frequency of spontaneous constrictions which occur in the smooth muscle and cause lymph propulsion. Studies on vascular endothelium have confirmed that there is great heterogeneity in the agonist-induced electrical responses of endothelial cells. Spontaneous transient depolarization activity was decreased with indomethacin (von der Weid et al., 1996). The decrease in spontaneous depolarization activity was not observed after lysis of the endothelium. The endothelium releases the prostanoids that activate vessels pumping. In guinea-pig lymphatic vessels, the primary factor released by the endothelium after application of acetylcholine (Ach) is the *endothelium-derived nitric oxide* (EDNO) that inhibits lymphatic pumping by activation of cGMP-dependent mechanisms in the smooth muscle, leading to a decrease in the size of the pacemaker currents, an increase in membrane conductance and a smooth muscle hyperpolarization (von der Weid et al., 1996). Histamine increased the frequency and amplitude of spontaneous transient depolarization; serotonin hyperpolarized the smooth muscle, causing a decrease in spontaneous transient depolarization activity. In effect, the serotonin on perfused lymph vessels inhibits constrictions in sheep mesentery (Hollywood et al., 1993).

Demonstration of the presence of gap junctions at the level of myoendothelial bridges in blood vessels (Spagnoli et al., 1982) suggests that transmission may also occur by electrical coupling. Functional evidence for this comes from electrophysiological

studies. In pig coronary arteries, action potential-like depolarizations and an isoprenaline-induced hyperpolarization generated in the smooth muscle, were simultaneously recorded in the endothelium, with the latter response abolished in the presence of the gap junction uncoupler halothane (von der Weid and Beny, 1993; Beny and Pacicca, 1994). Patch clamp recordings from the endothelium of intact rat aortae revealed membrane potential oscillations related to the response of the underlying smooth muscle to phenylephrine (Marchenko and Sage, 1994). In isolated arterioles of the hamster cheek pouch, both endothelial and smooth muscle cells were depolarized by phenylephrine, although α-adrenoceptors were present only on smooth muscle. Experiments of dye coupling between the smooth muscle and endothelium and vice versa, while not demonstrating heterocellular coupling in arteries and arterioles in situ when the anionic dye Lucifer Yellow was injected (Segal and Beny, 1992), did demonstrate endothelium to smooth muscle (but not smooth muscle to endothelium) dye coupling in arterioles when other low-molecular-weight dyes were used (Little et al., 1995). The extent of functional electrical coupling between smooth muscle and the endothelium in lymphatic vessels is still not clear. In previous studies, in open segment of guinea-pig mesenteric lymphatic vessels, the resting membrane potential (RMP) of the lymphatic endothelium resulted particularly negative (-71.5 ± 0.5mV) and significantly different from the value of -60.8 ± 1.1 mV recorded in smooth muscle. A more negative membrane potential would enhance the driving force for Ca^{2+} entry through any Ca^{2+} permeable channel. However, the functional electrical coupling between the endothelium and the smooth muscle has not yet been found (von der Weid and Van Helden, 1997).

1.9.1 Chemical modulation of the lymphatic function

Lymph flow increases during inflammatory reaction. Inflammatory mediators are involved in the modulation of lymphatics contractility. It is difficult, especially *in vivo,* to determine whether a lymphatic response is due to a direct stimulation by inflammatory mediators or it is a consequence of edema and vessel filling. Probably the effect is combined. The role of the lymphatic endothelium as a barrier between the lymph and interstitial compartments is little understood. The inflammatory signals may induce permeability increases. Different inflammatory cytokines and signalling molecules (Tumor necrosis factor alpha, interleukins-6 and -1 beta, interferon gamma, lipopolysaccharides) induce, in effect, endothelial barrier dysfunction (Cromer et al., 2013). During inflammation, the pathological levels of nitric oxide (NO) production may alter the barrier function. NO production is a major regulator of pumping activity of lymphatic vessels and its production may maintain the barrier integrity.

Systemically administered *histamine* produced increases in lymph flow (Lewis and Winsey, 1970; McNamee 1983) due to increased microvascular permeability (Haddy et al., 1972; Svensjo et al., 1982). Pre-treatment with H_1-antagonist suppressed the increase in lymph flow and protein concentration, suggesting that the increase in lymph flow caused by stimulation of H_1-receptors was affected by the increase in lymph formation (Dobbins et al., 1981). On contrary, histamine produced a lymph flow decrease when delivered to the thoracic duct of dog through *vasa lymphorum*. On rat mesenteric lymphatic vessels, histamine caused increases in vessel diameter and contractility, but not in contraction frequency (Ferguson et al., 1988). Because histamine is also present in the interstitium during the inflammation, it could directly stimulate lymphatic vessels function (Edery and Lewis, 1963).

Serotonin or 5-hydroxytryptamine (5-HT) is involved in changes in blood flow, vascular permeability and microcirculation (Plaku et von der Weid, 2006). In isolated bovine mesenteric lymphatics it stimulates tonic contractions (Ohhashi et al., 1978; Williamson, 1969). Contractions due to serotonin were studied in canine thoracic ducts and in porcine tracheobronchial and hepatic vessels (Takahashi et al., 1990; Ferguson et al., 1993; Hashimoto et al., 1994). When the vessels were pre-constricted, serotonin causes relaxation (Miyahara et al., 1994). The contractions were mediated by 5-HT_2 receptors, on the other hand, the relaxations were mediated by 5-TH_4 receptors, located on the smooth muscle of the lymphatics wall (Dobbins,1998; Miyahara et al., 1994).

Acetylcholine causes relaxation of the pre-constricted dog thoracic ducts and tracheobronchial lymphatics and induces a slowing of spontaneous constrictions in bovine, porcine and guinea- pig mesenteric lymph vessels and in afferent lymph microvessels from rat iliac lymph nodes (von der Weid et al., 1996; Ohahashi and Takahashi, 1991; Mizuno et al., 1998). These effects were mediated by the endothelial release of nitric oxide that abolishes spontaneous constriction cycles through arresting intracellular calcium release associated with spontaneous transient depolarizations and contractions. Nitric oxide-synthase (NOS) inhibitors increase the vessel contraction (von der Weid, 1996).

Inhibitors of cyclo-oxygenase (COX) and other arachidonate metabolism pathways on lymphatics, suppress their spontaneous contractile activity (Johnston and Gordon, 1981; Johnston and Feuer, 1983) suggesting that lymphatic vessels may be capable of generating arachidonate products in order to modulate their spontaneous activity. Application of leukotrienes, as well as a PGH_2/thromboxane A_2 (TXA_2) mimetics, induces rhythmic constriction in non-contracting vessels. These effects were blocked by

indomethacin. When PGH_2/TXA_2 receptors were blocked by antagonist, the constriction were converted to dilations (Mizuno et al., 1998).

The presence of cholinergic, adrenergic nerve fibers and peptidergic innervation have been demonstrated in guinea-pig and bovine mesenteric lymphatic vessels (Alessandrini et al., 1981; Ohhashi et al., 1982 (Guarna et al., 1991; Ohhashi et al., 1983). *In vitro*, VIP inhibits mesenteric lymphatic pumping (Ohhashi et al., 1983); CGRP also caused a decrease in lymphatic contraction frequency in the guinea pig mesentery. In the rat mesentery, CGRP enhanced phasic contractions of the lymphatic vessels (Akopian et al., 1998). The neuropeptide could cause an increase in the pacemaker activity in guinea pig mesentery; substance P increased spontaneous contraction rate (Foy et al., 1989).

There are studies on the effects of *alpha 1*- and *alpha 2-adrenergic* stimuli on rat mesenteric collecting lymphatics *in vivo*, monitoring mesenteric collecting lymphatic diameter by using a computerized video tracking system, and indexes of lymphatic pumping (e.g., contraction frequency, stroke volume, ejection fraction, and muscle shortening velocity). Contractile activity was monitored before and during the administration of various adrenergic agonists and antagonists. In particular, the receptor antagonists prazosin (alpha 1) and yohimbine (alpha 2) did not significantly alter lymphatic vessels tone or contractile activity, which suggests that lymphatics possess no basal adrenergic tone. Norepinephrine and phenylephrine produced dose-dependent increases in frequency and in lymphatic pump flow (the stroke volume did not change), and decreases in diameter. The changes in lymphatic pumping produced by norepinephrine were blocked by prazosin or phentolamine and only partially blocked by yohimbine. All these data suggest the existence of alpha-adrenoceptors on lymphatic smooth muscle (Benoit, 1997).

1.9.2 Epinephrine modulation

There is a great variability in the responses of lymphatic vessels to drugs, in particular to catecholamines. Injection of epinephrine into rat mesentery was followed by a contractile spasm of the lacteals in some vessels, and an increased rate of contraction in others, while other vessels did not respond (Florey, 1927). Epinephrine injected in testicle of rat and guinea pig caused an evident contraction of the trunks, due to the presence of smooth muscle-fibers, but this effect was not observed in cat and rabbit (Pullinger and Florey, 1935). The capillaries on the surface of the testis of cat were inactive to any stimuli. Epinephrine in a first experiment and epinephrine mixed with hydrokollag in the other, were injected in peritoneal cavity of rabbits. The hydrokollag injected into the peritoneal cavity filled the capillaries and trunks, on the diaphragm pleural surface (Florey, 1927). This procedure did not reveal significant contractions. Epinephrine and pituitrin caused either lymphatic spasm and an increased contractile rate, or only a change in rate (Figure 1.17, Smith, 1949).

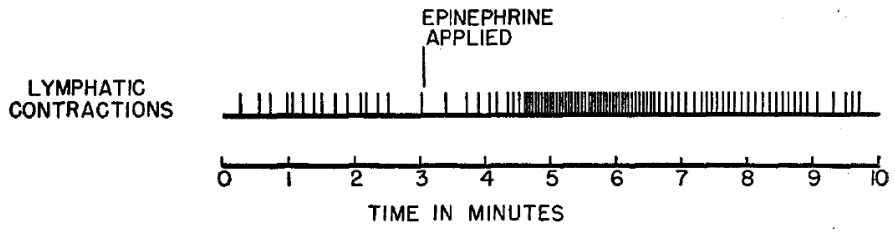

Figure 1.17. Effect of topical application of epinephrine on lymphatic contractile rate (Smith, 1949).

Epinephrine increases skeletal muscle blood flow and this may be accompanied by an increase in lymph production and flow (Allen et al., 1946). Intravenous infusions of epinephrine and norepinephrine increase thoracic duct lymph flow in many animals (Shim et al., 1961; Doemling and Steggerda, 1962; Fujii and Wernze, 1966; Schad and

Brechtelsbauer, 1977) due to an increased lymph production rather than a direct effect on lymphatic contractility. Hall, Morris and Woolley (1965) found that the epinephrine had no effect on thoracic duct pressure or lymph flow in sheep. Norepinephrine depressed thoracic duct flow in the dog while epinephrine enhanced it (Foldi and Zoltan, 1966). In contrast, De Micheli and Glasser, in 1975 have demonstrated that both epinephrine and norepinephrine increased thoracic duct flow in dogs (De Micheli and Glasser, 1975), accompanied by a fall in blood flow and venous pressure and lymph formation. Norepinephrine and epinephrine have a direct action on lymphatic smooth muscle, increasing the fluid propulsion, in certain doses and in certain conditions. It is possible that the effect of this drugs also depends on transmural pressures (McHale and Roddie, 1976). Norepineprhine increases the spontaneous contraction frequency of isolated bovine lymphatic vessels, but reduces contraction force by disruption of spontaneous pacemaking rather than by any direct effect on vessel contractility (Allen et al., 1983). Norepinephrine had effect of increasing the frequency of longitudinal contraction of isolated segments of bovine mesenteric lymphatic. Epinephrine and norepinephrine infusion has been shown to increase the frequency and force of lymphatic pumping in sheep (McHale and Roddie, 1983), causing a significant increase in lymph flow but this caused no change in lymphocyte subset distribution, leukocyte concentration, or pool of lymphocytes; the increase was followed by a post-injection decrease in flow and cellular output (Seabrook et al., 2001). Lymph flow was also measured in popliteal, prefemoral and mesenteric lymphatic vessels in conscious sheep. Intravenous epinephrine infusion increased frequency of lymphatic contraction and lymph flow in all three vessels. In particular the prefemoral vessels flow remained high after the infusion had stopped, on the other hand with norepinephrine prefemoral flow was depressed but also the contraction frequency and the lymph flow were increased

(McHale and Roddie, 1983). Epinephrine may cause an increase in lymph flow by either acting directly on the lymphatic vessels, reflexively triggering the autonomic nervous system, or increasing blood flow to the region drained by the lymphatic vessels (McHale and Roddie,1983).

2. *State of art and Aim*

2. State of art and Aim

In a recent study, performed in our laboratory, it was found that in the same loops the flow direction not always followed intraluminal average pressure gradients but it was able to revert multiple times with an average frequency of circa 4 times per minute. In these vessels lymph progression is oscillatory, both simultaneously or in sequence in the same and/or different tracts of the same loop, not dependent on cardiac or respiratory frequency. Intraluminal gradients between adjacent lymphatic segments revert multiple times in adjacent vessel tracts, thus suggesting the presence within the loop of numerous intraluminal valves able to control lymph flow direction. We have been able to describe the lymphatic intraluminal valves in both linear vessels and loops, and lymph flow has been estimated by measuring the motion of microspheres suspended in the lymph. The aim of our study was to investigate, in actively contracting sites of peripheral diaphragmatic lymphatic vessels, the contribution of single strokes on the local lymph flow witnessed by microsphere progression and valve opening/closing dynamics upon lymph propulsion, and the modulation of flow following epinephrine administration.

3. Materials and Methods

3. Materials and Methods

3.1 In vivo and ex vivo experiments

The experiments were performed on adult Wistar rats (mean body weight: 414 ± 146g n=9) following the procedures and experimental protocols approved by ethical research committee of the Insubria University, Varese. Animals were anaesthetised with a cocktail composed of 75 mg/Kg ketamine (Imalgene© 1000, Merial, Italy) and 0.5 mg/Kg medetomidine (Domitor©, Pfizer); ketamine half-boluses were administered every hour. Rats were euthanized via an anaesthesia overdose, at the end of the experiments. The disappearance of the corneal reflex allowed to control, during the experiment, the maintenance of a deep surgical anaesthesia level. After that, the rats were turned supine on a warmed (37°C) blanket and were then tracheotomised with a T-shaped cannula inserted into the trachea. The diaphragmatic lymphatic vessels were *in vivo* stained by an intraperitoneal injection of 2% FITC-dextran (FD25OS-Sigma Aldrich, Italy) in saline plus 10% microspheres (F8813-FluoSpheres Carboxylate-Modified Microspheres, 0.1 – 1 μm, Yellow-Green Fluorescent (505/515), Invitrogen). After 1 hour of staining in the prone position, the animals were paralysed with a bolus of 0.3 ml pancuronium bromide (Sigma Aldrich, Milan, Italy) solution (2 mg/ml in saline) administered in the exposed jugular vein. Immediately after paralysis, the tracheal cannula was connected to a mechanical ventilator (model Inspira SV DCI-7058, Harvard Apparatus, USA), and rats were ventilated in room air with a tidal volume and frequency automatically set by the ventilator on the basis of rat weight. Then, the chest wall was opened, the caudal four to five ribs were removed, the pleural diaphragmatic surface was exposed and the stained lymphatic network was visualized. Warm saline solution was flushed on the diaphragmatic surface in order to avoid

dehydration. Specimens of diaphragm were excised and superfused with oxygenated Tyrode's solution, of the following composition (mM): 119 NaCl; 5 KCl; 25 HEPES free acid; 2 $MgCl_2$; 2 $CaCl_2$; pH: 7.4, kept in a flow chamber on the stage of an upright microscope (BX51, Olympus) equipped with a black-and-white Watek camera connected to a personal computer running VirtualDub software. Images were collected at 10 Hz to optimize the spatial and temporal resolution of the contracting vessels kinetic and lymph flow. Microspheres movements were video recorded *ex-vivo* in control conditions and during administration of epinephrine 20 µM prepared from a 20 mM stock solution (E-4375, Sigma Aldrich, Italy) in Tyrode's solution, and perfused, through a pipette connected to a manipulator, on the diaphragm specimen located inside the flow chamber.

3.2 Time dependent changes of lymphatic vessel diameter

Diameter analyses can be performed manually, but this approach is time-consuming and allows only a small number of images to be processed (Simons et al., 1987). Initially, light microscopy with graded eyepieces was used, and then video microscopy allowed taping and analysis along scan lines (Intaglietta and Tompkins, 1972; Halpern and Kelley, 1991). Later analysis of multiple sites of interest was performed on digital images online and offline (Yip et al., 1991; Lee et al., 2009). For automatic measurement commercial solutions are available, but the proprietary algorithms and their shortcomings are not known to the user. Automatic diameter analysis was reported for coronary angiography, b-mode ultrasound, CT and MRI data (Vas et al., 1985; Hoogeveen et al., 1999; Beux et al., 2001; Andriotis et al., 2008). AVI video format was converted into TIFF stacks with ImageJ software (NIH), and stabilized with built-in

ImageJ plug-in. The diameter of the observed lymphatic vessels was measured over time using “Diameter” plug-in of ImageJ software. This plug-in uses an algorithm to estimate the inner vessel diameter based on the FITC-fluorescent dye filling the vessel. The diameter of the selected vessel is measured five times for the loaded image or image stack. In order to measure the vessel diameter during the entire time stack, in spite of residual lateral movements of the vessel, the maximum intensity projection of the time stack was used as a template to correctly position the diameter-measuring line perpendicularly to the vessel major axis. In effect, the algorithm requires a line selection by the operator. This should cross the vessel and exceed the maximum vessel diameter during the investigated period on both sides. This is why ROIs were plotted on the z-stack maximum projection image. The “Dynamic Profiler” function of ImageJ showed the pixel intensities profile in real time. The boundary estimates (a1 and a2 in Figure 3.1) are the two positions with the maximum difference between the mean intensity of the three adjacent points to both sides. This separates the profile in three parts. Reference intensities (b1, b2 and b3) are the dark areas outside the lymphatic vessel, separately for both sides, and the darkest area within the vessel, determined by the average of three consecutive points. The intensity threshold (c1 and c2) is the average of the adjacent reference intensities, calculated separately for both sides to account for different surroundings of the vessel. The intensities of the two positions left and right of the boundary estimates are fitted with a linear trend. The point of intersection (d1, d2) of the fit with the intensity threshold gives the precise vessel boundary. A pipe has half of its maximal thickness at sqrt (3/4) of the radius; therefore the diameter of the vessels is [d1,d2] * sqrt (4/3). The diameter and both ends of the full width at half-maximum of the vessel (in pixels) of the five adjacent measurements and for every loaded image are copied to the system clipboard (Fisher et al., 2010).

The mean value of diameter measurements was transformed to the corresponding microns value and then plotted vs time using Origin 5.0 Software. Results were then analysed through a Clampfit 10.2 Software free sheet, setting the correct sampling frequency (10 Hz).

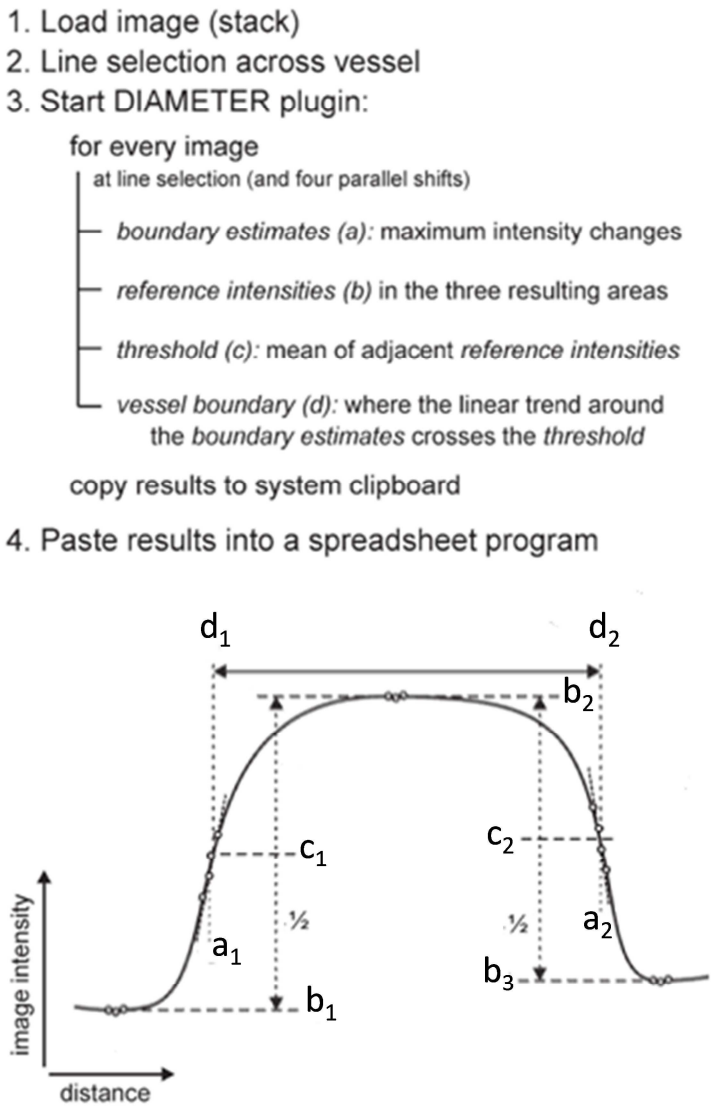

Figure 3.1. Steps 1–4 are the work of the human observer. The flowchart lists the intermediate results (a–d) calculated by the algorithm for every image of the loaded stack. (Fisher et al., 2010).

3.3 Microsphere progression in lymphatic vessel

In order to follow the microsphere progression, their movement was followed over time using “Manual Tracking” plug-in of ImageJ software. Before tracking *xy* calibration value as well as the time interval value have been set in the appropriate option boxes. The results table shows recorded *xy* coordinates, the distance travelled by the microsphere during the time interval between two successive images, and velocity of movement. The sign of the distance value traveled by the microsphere has been assigned considering the lymph flow direction averaged over several minutes. After choosing the microsphere to follow, we have assigned a positive sign when it was pushed, within the lymphatic vessel, along the net lymph flow direction, instead a negative sign when the microsphere was pushed against the mean bulk flow direction. The value of distance and velocity were analyzed with Microsoft Excel Software to create the distance vs time and velocity vs time plots.

3.4 Velocity profile of microspheres

By using of the Manual Tracking plugin of ImageJ software, we measured the velocity profile of the microspheres along the transverse axis of lymphatic vessels in order to obtain data regarding the type of flow that lymph displays. Indeed, should the flow be laminar, we expect to find a parabolic velocity profile (Figure 3.2). The values of lymph flow velocity and the microsphere position were analyzed with Microsoft Excel Software to create the lymph flow velocity vs x axis position plots.

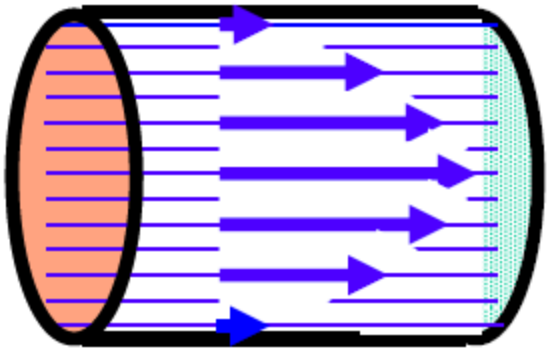

Figure 3.2. Parabolic velocity profile. The velocity is maximum at the center and gradually decreases in the vicinity of the walls of the vessel.

3.5 Cross sectional area measurement of lymphatic valves

By using the Manual Tracking plugin of ImageJ software, the velocity of microspheres flowing inside the lymphatic vessel and through the valve has been measured. Based on the continuity principle ($J_v = A_i \cdot v_i$), assuming a stationary flow rate, from the comparison of the velocity of the microsphere when it flows through the valve with respect to its velocity in the valve flanking regions of the vessel, we were able to estimate the cross section of the lymphatic valve expressed as percentage of the cross sectional area of the flanking regions of the vessel (Figure 3.3). The cross sectional areas of the valve flanking regions (A_U and A_D in figure 3.3) have been averaged together (and also the respective microsphere velocities measured in the same positions) to give a mean cross sectional area in order to derive flow rate from the averaged microsphere velocity.

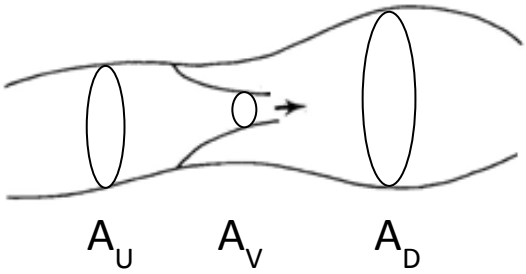

Figure 3.3. Representation of the valve, upstream and downstream tracts to estimate the valve cross sectional area (NA_V). A_v: valve area; A_u: upstream area; A_d: downstream area. The arrow represents the lymph flow direction.

3.6 Micro-injection

In order to verify the presence of valves open or closed in diaphragmatic lymphatic vessels and to understand the lymph flow direction, we prepared, using a P-97 Flaming/Bown type Micropipette Puller (Sutter Instrument, Novato, USA), glass pipettes for microinjection from borosilicate glass capillaries (1B100-4, 1.0 mm outer diameter, 0.78 mm inner diameter, WPI Europe, Berlin, German) with tip diameters of ~ 25 μm and then they were beveled in order to reduce the damaging impact when piercing the vessel wall. Pipettes were back-filled with mineral oil and mounted onto a mechanical microinjector (WPI Europe) set to delivery 9.2 nl/injection, at an injecting rate of 10 nl/sec. Pipette were front filled with 1μl of TRITC-dextran 2%. With the use of a mechanical coarse/fine micromanipulator (Narishige), the pipette was placed next to the vessel to be injected and advanced through the pleural diaphragmatic surface until it was inside the lymphatic vessel lumen where was triggered a single injection of 9.2 nl of TRITC- dextran 2%. The phases of pipette positioning, fluorescent dye injection, and distribution of the dye into the lymphatic vessel lumen were recorded by the upright microscope (BX51) which was equipped with a cooled black-and-white charge-couple

device camera (Watek) connected with a personal computer running VirtualDub software.

3.7 Statistical analysis

The statistical analysis was performed using Origin 5.0 Software. Data are presented as mean ± SE. Differences between means were considered significant at $p < 0.05$. Statistical significance of the differences between mean values was computed using paired *t*-test.

4. Results and Discussion

4. Results and Discussion

4.1 Diaphragmatic lymphatic vessels visualization

Not stained lymphatic vessels are characterized by a darker-than-surrounding lumen lined by white borders. The diaphragmatic lymphatic network can be visualized both in white epi-illumination and fluorescence after peritoneal dye injection (Figure 4.1). This last method allows to visualize a larger number of vessels, to measure the lymphatic vessel diameter length and to study the lymph flow.

Figure 4.1. Stereomicroscope image of diaphragmatic lymphatic loops. The lymphatic loops, situated on the pleural surface of the diaphragm, were acquired after FITC-dextran intraperitoneal injection. Scale bar: 500 μm.

The FITC-dextran freely moves within the vessel and its smaller collaterals without going out of the wall. In our experiments, diaphragmatic lymphatic vessels were found not to be permeable to extravasation of FITC-dextrans (~11 nm in hydrodinamic radius, Armstrong et al, 2004, Lee et al., 2010) and microspheres mix. After 1 hour of incubation and during the video recording, no fluorescent dye extravasated from the vessels lumen. Conversely, mesenteric lymphatics, vessels extensively studied, were found to be leaky to FITC- albumin (~4nm in hydrodinamic radius) (Unterberg et al.,

1984), acting as exchange vessels which are able to extravasate solute and filter fluid (Scallan and Huxley, 2010). We have chosen the intraperitoneal injection of dyes to *in vivo* staining the lymphatic vessels since already 30 minutes after the peritoneal injection, ~90% of the dye can be found filling even pleural lymphatics when imaged from the pleural side. Moreover, a smaller volume of the FITC dye can be injected in the pleural space, because it may compromise the respiratory function. The dextrans have properties such as density and viscosity, similar to the lymph, and the initial lymphatics allow solutes larger than 70 KDa, as the dextrans fluorescent, to cross the vessels wall. They are mixed with the intraluminal fluid and the primary valves confined the dextrans in the vessel lumen preventing dye backflow through the vessel wall. The TRITC labeled microspheres used to study and follow the lymph flow have a diameter useful to have less friction with the vessels wall and to allow the crossing of any valves. This staining allowed us to observe very well the *lymphatic lacunae* (Figure 4.2 A) and we also recognized presence of *vasa lymphorum* (Figure 4.2 B) within the well-developed media of the same lymphatics. The lacunae, located within the interstitial space under the mesothelial layer, are in continuity with the lymphatic vessels which run perpendicular to the lacunae and through the skeletal muscle fibers. The vasa lymphorum may be essential for maintaining the vigorous rhythmic contractions of the lymphatic smooth muscles which act as driving force for the propulsion of lymph and may contribute to the modulation of intrinsic contractility due to epinephrine and other modulatory molecules conveyed to the lymphatic smooth muscle cells.

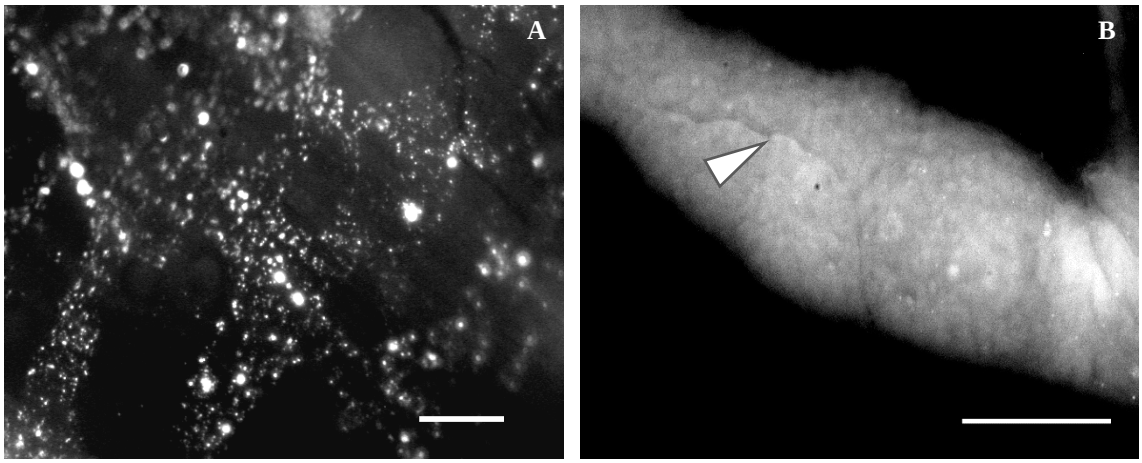

Figure 4.2. Images after a FITC-dextran with TRITC-microsphere injection. A. TRITC-emission**:** *lymphatic lacunae* **B**. FITC-emission: *vasa lymphorum* **(**white arrowhead**).** Scale bar: 150 μm.

Analyzing the microspheres progression that mimes the lymph flow, a great variability has been found among all lymphatic vessels. In some tracts, the lymph goes unidirectionally (figure 4.3, green trace), in other it goes forward and backward (yellow, purple and white traces). This confirms that the lymph flow reverts multiple times its direction in the same vessel.

In the same loop, the flow trend was very variable, suggesting the presence, within the vessel lumen, of numerous lymphatic valves and of musculature involved in the lymph flow direction changes.

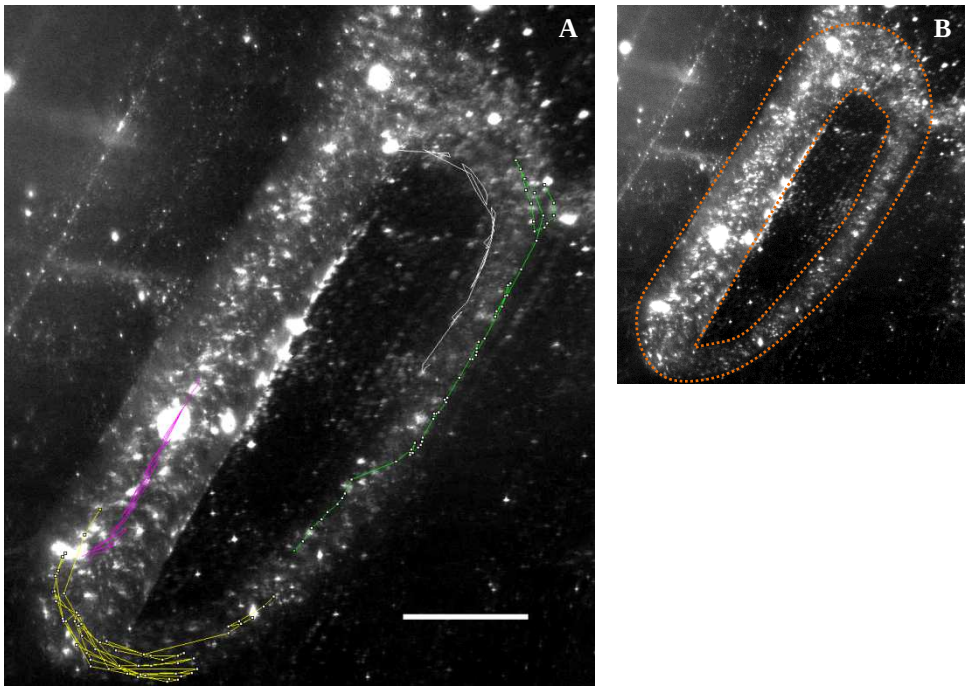

Figure 4.3. TRITC - emission in a lymphatic loop. A. The different microspheres trajectory along the same lymphatic diaphragmatic loop (represented in **B** insert) obtained with Manual Tracking plugin. Scale bar: 250 µm.

4.2 Localization of intraluminal lymphatic secondary valve

It was possible to distinguish within the loop and linear vessels the intraluminal valves, to study their dynamic properties in relation to muscle contraction and their role in shaping lymph propulsion. The presence of interconnected linear vessels and loops creates a very complex network whose physiological properties are difficult to study. The network in figure 4.4 was obtained with an images collage, through the Abobe Photoshop software, acquired by a fluorescence microscope. Different regions of the same network showed different behaviors, in particular we investigated the active pumping tracts with an intraluminal valve, as the loop indicated by red arrowhead.

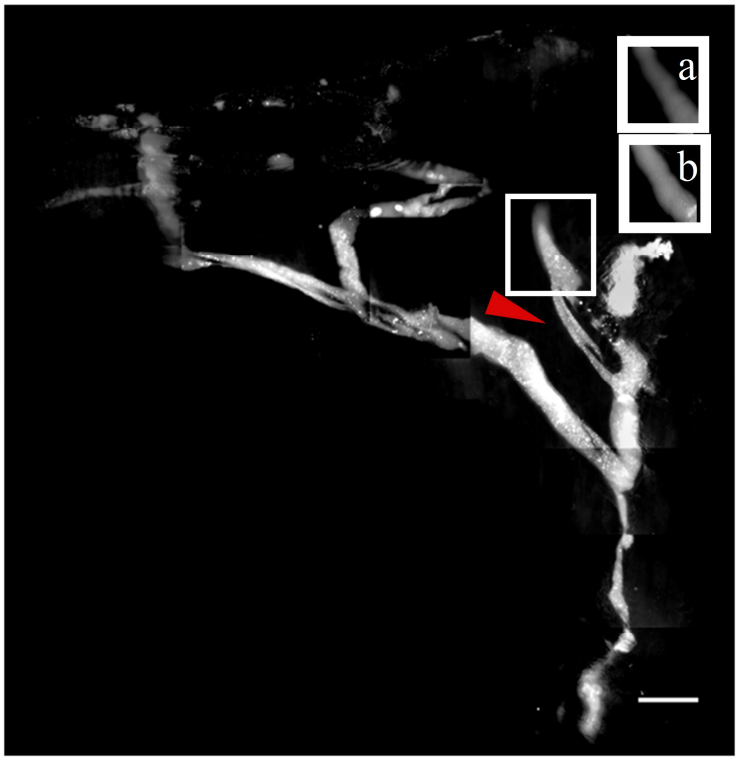

Figure 4.4. Lymphatic diaphragmatic network. The red arrowhead shows an active pumping loop with an intraluminal valve. Insert **a** represents the contracted state of the lymphatic loop; **b** site in a not contracted state. Scale bar: 250 μm

The complex loop depicted in figure 4.5 is the example from which data plotted in figure 4.7 have been derived. The state of the valve is indicated by the coloured triangles (red for closed valve, green for open valve), dotted white lines are superimposed on the two sites from which the diameter plots of figure 4.7 have been measured, while the blue asterisk indicates the position of the microsphere whose track has been plotted in figure 4.7. Asterisks in figure 4.5 indicate when that site is in a contracted state. We observed that the contraction of the lymphatic tract above the valve, indicated by the white dotted line in figure 4.5A, induces the valve closure whereas the contraction of the right inferior branch, also indicated by the white dotted line on the right branch in figure 4.5A, forces the valve to open.

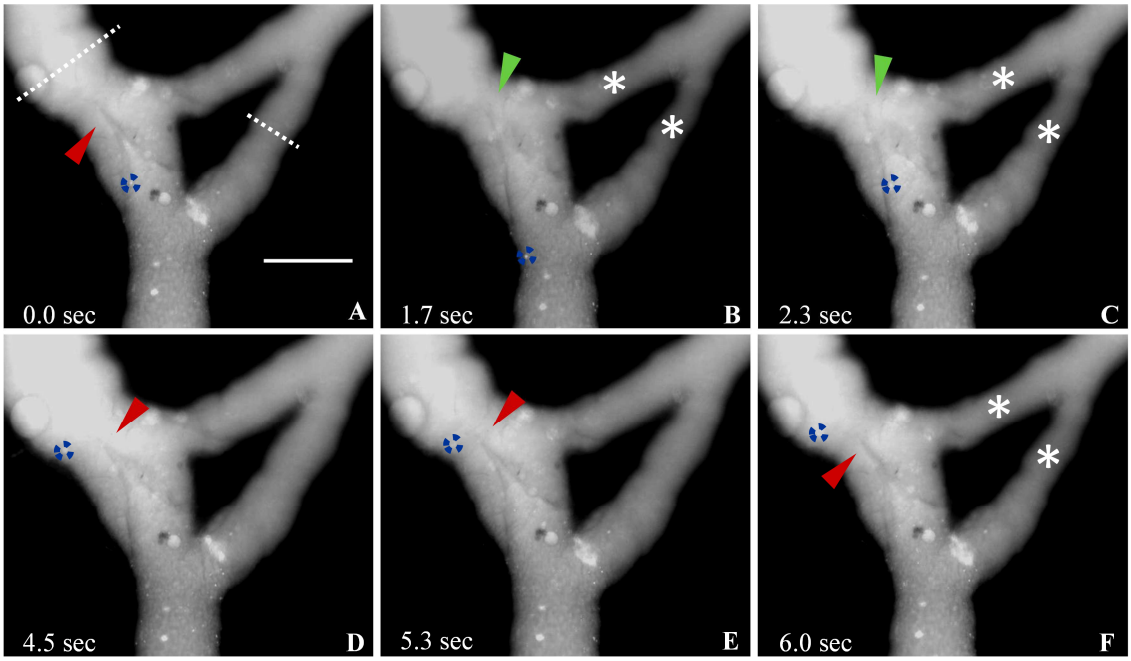

Figure 4.5. Intraluminal valve. Closed (red arrowheads in panels **A** and **D-F**) or open (green arrowheads in panels **B-C**) state. Blue dotted circles underline a single microsphere crossing the lymphatic valve. Asterisks indicate when that site is in a contracted state. Contraction of the lymphatic tract downstream the valve induced the valve closure, whereas the contraction of the right branch may have induced an increase in upstream intraluminal pressure, causing the lymphatic valve to open. Lymphatic vessels' diameters were measured at sites indicated by white dotted lines. Scale bar: 250 µm.

From the path followed by the microspheres when they move through the valve (figure 4.7C and D), like the one indicated by the blue asterisk in figure 4.5, we have been able to estimate the bulk flow direction from the mean slope of both trace. The result is indicated with the yellow arrow in figure 4.6.

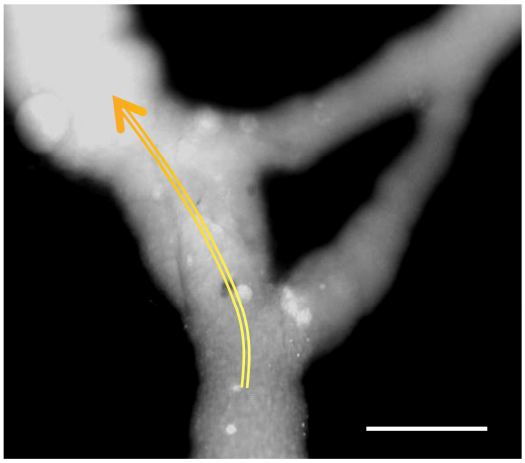

Figure 4.6. Diaphragmatic lymphatic loop analyzed in figure 4.5. Yellow arrow: net direction of lymph flow. Scale bar: 250 µm.

4.3. Cross sectional area of lymphatic valves

Since it was not possible to directly measure the functional cross sectional area of the valve when it was open, we derived this value by exploiting the continuity principle (see methods for details). We measured an average cross section of the lymphatic vessels flanking the valve of 4674.46 ± 159.35 μm^2 (n=3) and an average flow velocity in the same tracts of 81.53 ± 5.54 µm/sec (n=3). We thus calculated an average flux rate of 0.46 ± 0.06 nl/sec (n=3). From this value and the measured mean microsphere velocity when traversing the open valve (188,26 ± 16.94 µm/sec n=3), we derived a functional cross sectional area of the valve of 2440.5 ± 130.2 μm^2 (n=3), that is 52.2% of the vessel cross sectional area.

4.4 Intrinsing pumping and microspheres progression

Figure 4.7 shows changes over time of the diameter of lymphatic vessels simultaneously measured at two different sites of the loop depicted in figure 4.5. Panels A and B represent the plots of the diameter over time as measured in the two sites indicated by the dotted lines in figure 4.5A. Panels C and D represent the plots of microspheres progression over time. Zero distance represents the valve position. In C we considered the path traversed by microsphere of the diaphragmatic lymphatic vessel from the tract downstream the valve. During the diastolic phase microspheres proceed along the net direction of flow (cfr figure 4.6). Contraction of the lymphatic tract downstream the valve induced not only the valve closure but also pushes the microsphere against the bulk flow direction towards the closed valve; in D we have considered the microsphere progression in the tract upstream the valve of the diaphragmatic lymphatic vessel. Contraction of the lymphatic tract downstream the valve pushes the microsphere against the bulk flow direction, whereas contraction of the right branch causes the valve opening and the microsphere is forced along the net flow direction. Once crossed the valve, the microsphere unidirectionally flows away from the valve.

This observation confirms that the valve is modulated by the active contractions of the smooth muscle cells of the vessels wall. The periodic contractions of the lymphatic vessels permit the opening or closing of valves and promote and modulate lymph progression.

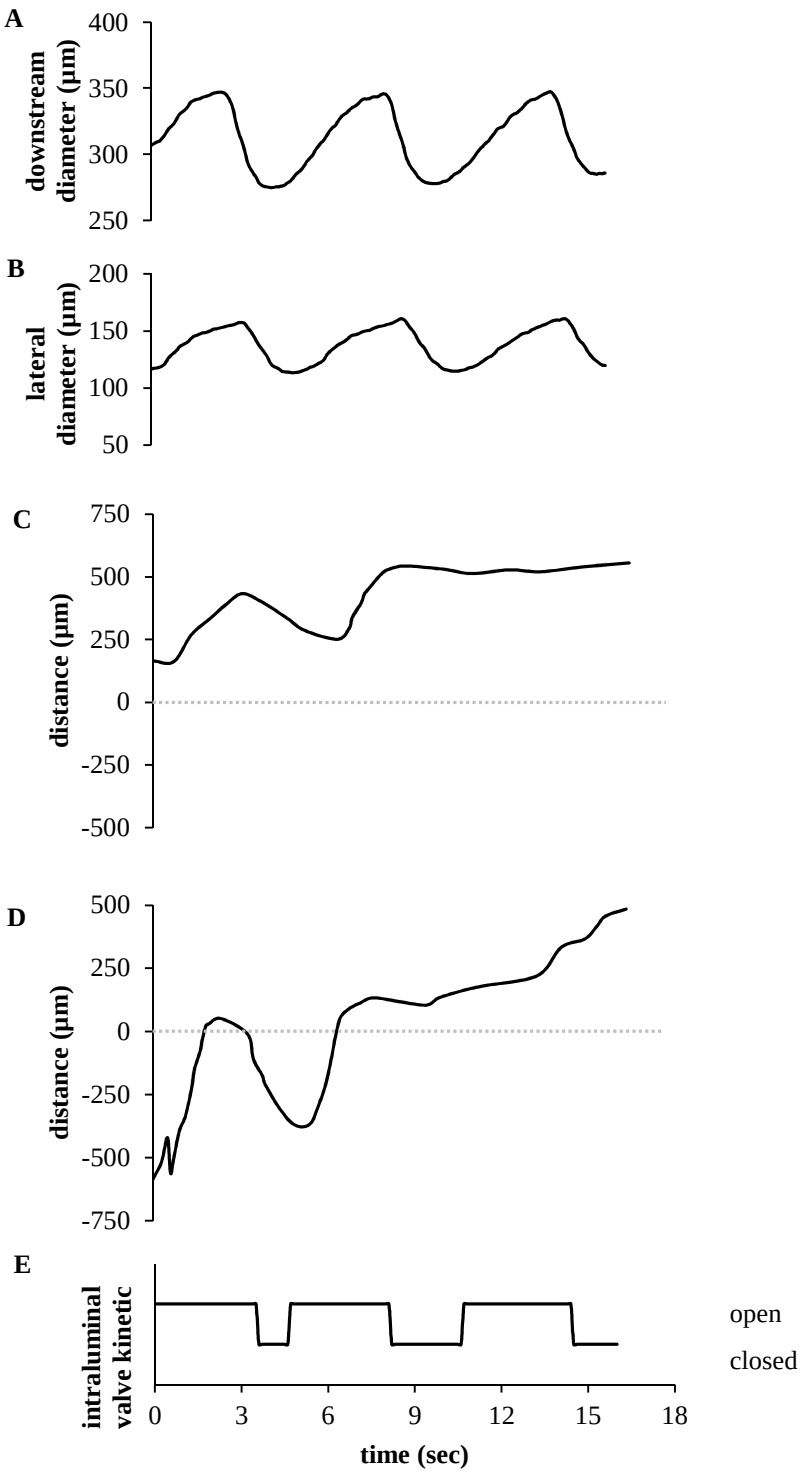

Figure 4.7. Diaphragmatic lymphatics diameter changes and microsphere progression. A. Changes over time of the diameter of the diaphragmatic lymphatic vessel of the downstream valve branch. **B. C**hanges over time of the diameter of the diaphragmatic lymphatic vessel right branch. **C.** Progression of microsphere of the diaphragmatic lymphatic vessel from the tract downstream the valve. *Zero distance represents the valve position.* **D.** Progression of microsphere in the tract upstream the valve of the diaphragmatic lymphatic vessel. **E.** Open/closed state of the lymphatic valve as derived from the video recording.

Microspheres, progressively more distant from the contracting site, undergo a displacement inversely correlated to their initial distance from contracting site (Figure 4.8).

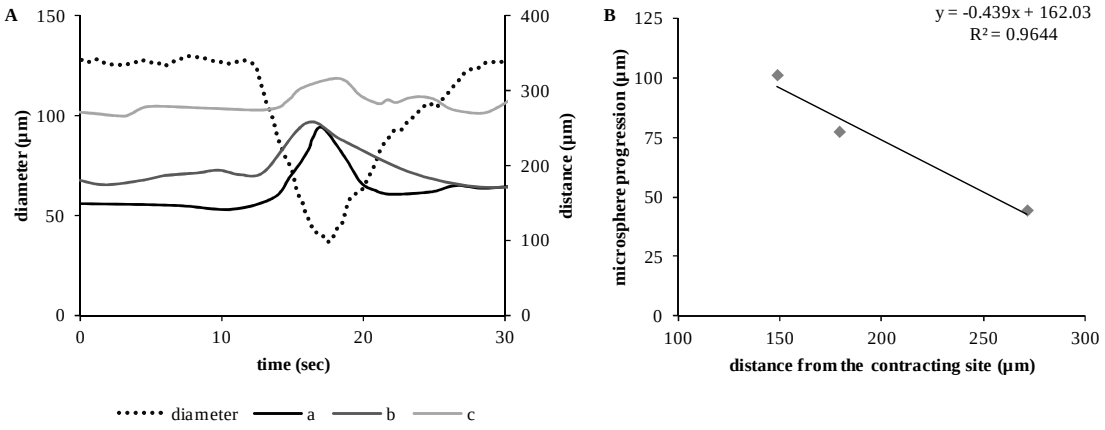

Figure 4.8. Diaphragmatic lymphatics diameter changes and microsphere progression in a lymphatic vessel without valve. A. Active stroke in a lymphatic diaphragmatic vessel without an intraluminal valve (grey dotted line). Microsphere distance from contracting site (represented by zero distance) vs time. Traces **a, b** and **c** refer to microspheres progressively more distant from the contracting site. **B.** Microsphere progression vs distance from the contracting site. The single point has been fitted by a linear trend

In the example depicted in figure 4.8, the microsphere closest to the contracting site undergoes a thrust greater than microspheres gradually more distant. In particular, the microsphere **a,** the nearest particle**,** undergoes a thrust of 101.18 µm; the microsphere **b** of 77.35 µm and the microsphere **c,** the farthest particle, of 44.33µm (Fig 4.8 B).

4.5 Parabolic profile of microspheres velocity

In order to investigate the flow regimen of lymph, we measured the velocity profile of different microspheres flowing inside lymphatic vessels that were lying along the transverse axis of lymphatic vessels. As shown in figure 4.9, data show that their velocity profile can indeed be fitted by a parabolic line, thus proving that, lymph in the vessels investigated flows in a laminar fashion. The velocity of central microsphere is 95.99 ± 11.49 μm/sec instead the velocity of microsphere nearest to wall vessels is 43.27 ± 7.15 μm/sec (n=4). The profile of the longitudinal velocity in the laminar flow assumes a parabolic profile (Figure 4.9).

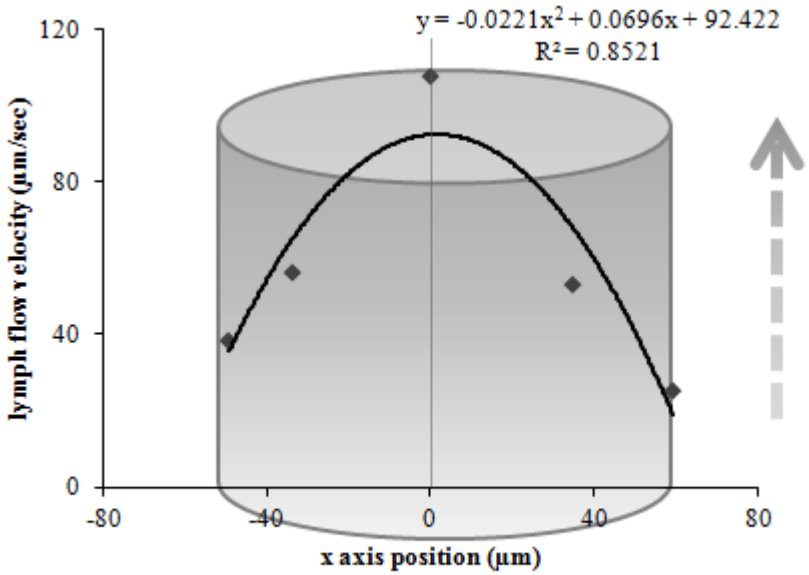

Figure 4.9. Lymph flow velocity and the microsphere position within the vessel lumen (represented by cylinder). The points can be fitted by a parabolic line whose equation is reported on the plot. The dotted arrow indicates the lymph flow direction.

4.6 The Lymphangion

We have also been able to investigate the temporal coordination between two adjacent lymphangions in a short linear segment connecting two lymphatic loops (figure 4.10). When the segment on the left contracts the segment on the right relaxes and then the opposite occurs (Figure 4.10 A, B. c and r letters refer to the contracted or relaxed state of the vessel segment close to the letters). The not simultaneous contraction of two lymphangions is evident in the figure 4.11. The plot represents the simultaneous recording of diameter changes (as measured at the dotted line positions in figure 4.10) in time in both lymphangions and the right most tract containing the valve (figure 4.11 trace c). During the systolic phase (characterized by a smaller diameter) on the left tract and the diastolic phase (characterized by a larger diameter) on the right tract, the microspheres are pushed forward along the lymph flow direction, that can be derived from the average slope of the dotted trace in figure 4.12. A valve is clearly visible only in the right portion of the vessel (panels E and F) which is not contracting (trace c). The valve when the microsphere is pushed forward is closed and the microspheres in this area do not move, as demonstrated also by the TRITC-dextran 2% micro-injection (Figure 4.13). The fluorescent dye remains confined on the right side of the valve, proximal to the injection site, and does not flow through it.

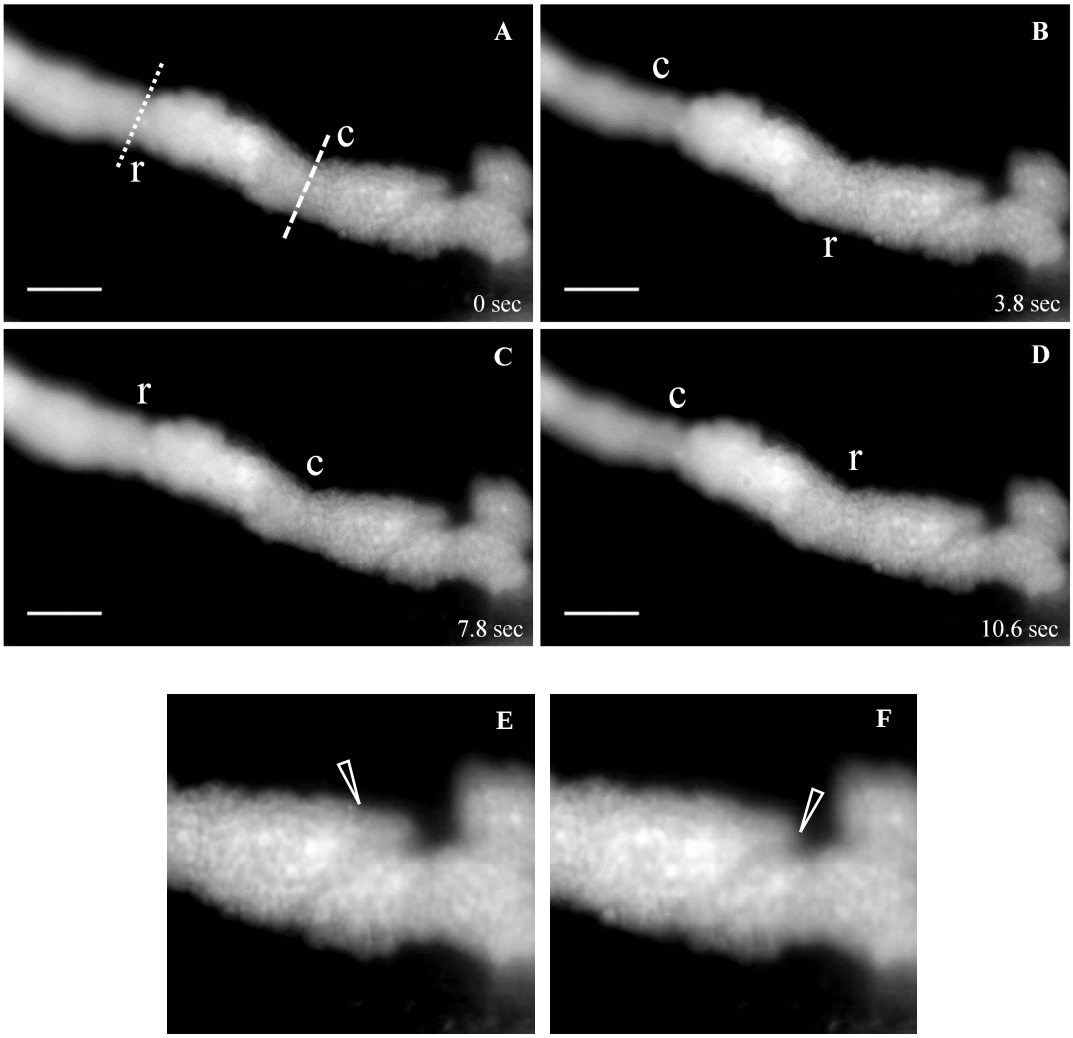

Figure 4.10. Lymphangions image sequence acquired after the fluorescent injection. The lymphangions contract (**c**) and release (**r**) in different moments. **A** and **C.** The diameter on the left, before the contraction, is ~108 μm and, after the contraction (**B** and **D**) is ~ 91 μm. Conversely, the diameter on the right (**A** and **C**) is ~78 μm because the lymphangion is contracts, whereas in **B** and **D** the lymphatic vessel is relaxed and its diameter is ~120 μm. Lymphatic vessels' diameters were measured at sites indicated by white lines. In the bottom left corner is shown the elapsed time recording from the beginning. **E.** Closed state of the valve (white arrowhead) or open (white arrowhead in panel **F**) state. Scale bar: 250 μm.

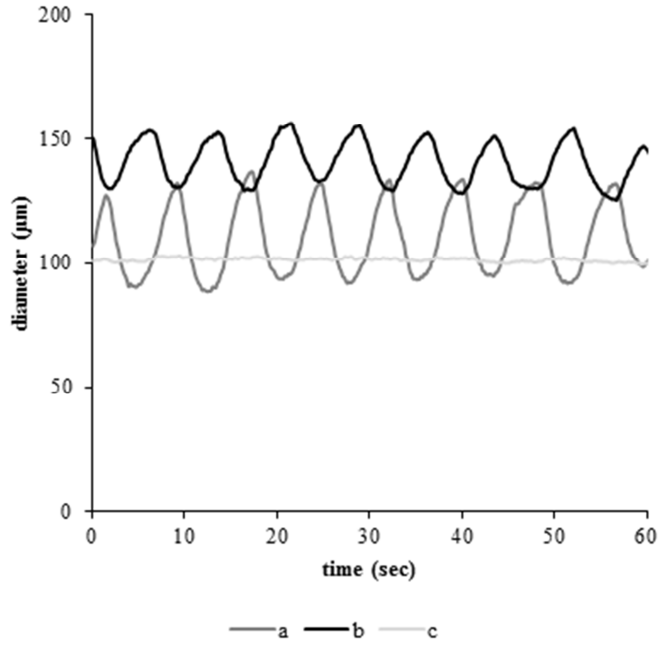

Figure 4.11. Simultaneous recording of diameter changes vs time profiles, in the lymphangions. Trace **a** refers to contractions of the lymphangion represented on the left in figure 4.10. Trace **b** refers to contractions of the lymphangion on the right. Trace **c**: invariant not contracting tract, corresponding to region downstream the visible valve. It is evident the not simultaneous contraction of two lymphangions.

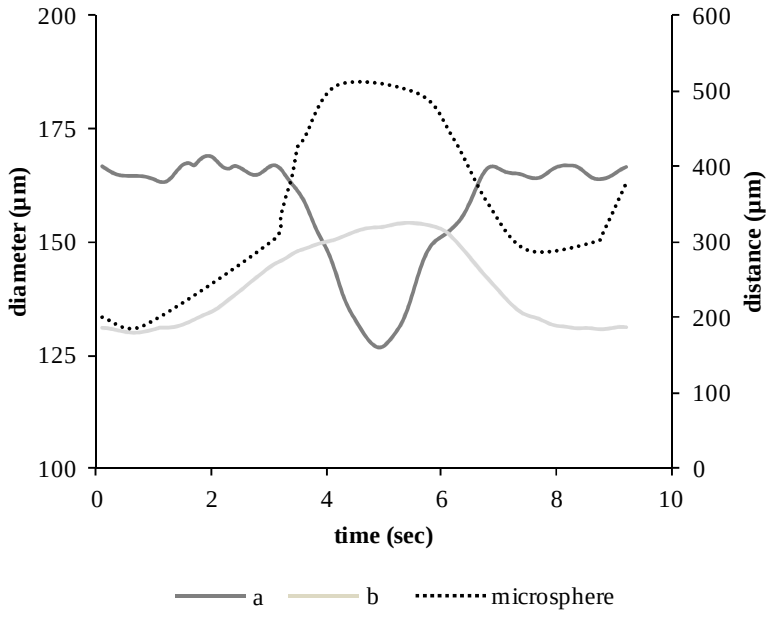

Figure 4.12. Diaphragmatic lymphatics diameter changes and microsphere progression. Active stroke in the lymphangion represented by white dotted lines in figure 4.10 (**a**). Simultaneously measured of the diameter changes on the other side represented by white dashed lines (**b**). Microsphere distance from contracting site (represented by zero distance) vs time (black dotted line). The microsphere undergoes a thrust due to contraction of lymphangion on the left.

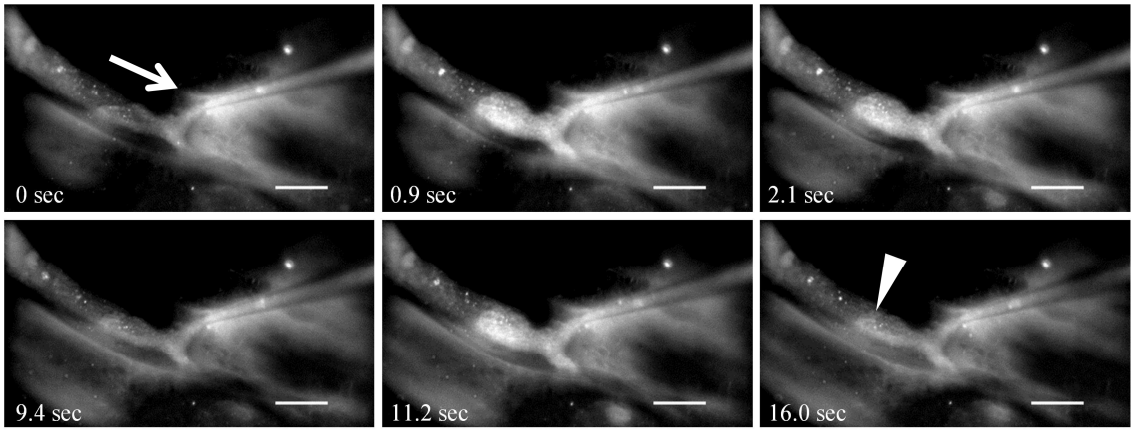

Figure 4.13. Image sequence acquired during the TRITC-dextran 2% micro-injection. In the bottom left corner is shown the time elapsed from the recording beginning. The TRITC-dextran was injected in the right side of the image indicated by white arrow, the dye progressed toward left but because the intraluminal valve (white arrowhead) is closed, the fluorescent dye remains confined in the area on the right. Scale bar: 150 μm.

4.7 Intraluminal valves in passive vessels

The secondary valves were found both between two active segments and between an active and a passive segment of lymphatic vessel (Figure 4.14). The passive vessels are characterized by enlargement due to contraction of the nearby lymphatic tract; in figure 4.15 upward deflection from the baseline value corresponds to passive vessel enlargement. The valve has two evident leaflets (left and right). Contraction of the lymphatic tract upstream the valve may have induced an increase in upstream intraluminal pressure, causing the valve opening and the lymph flow progression.

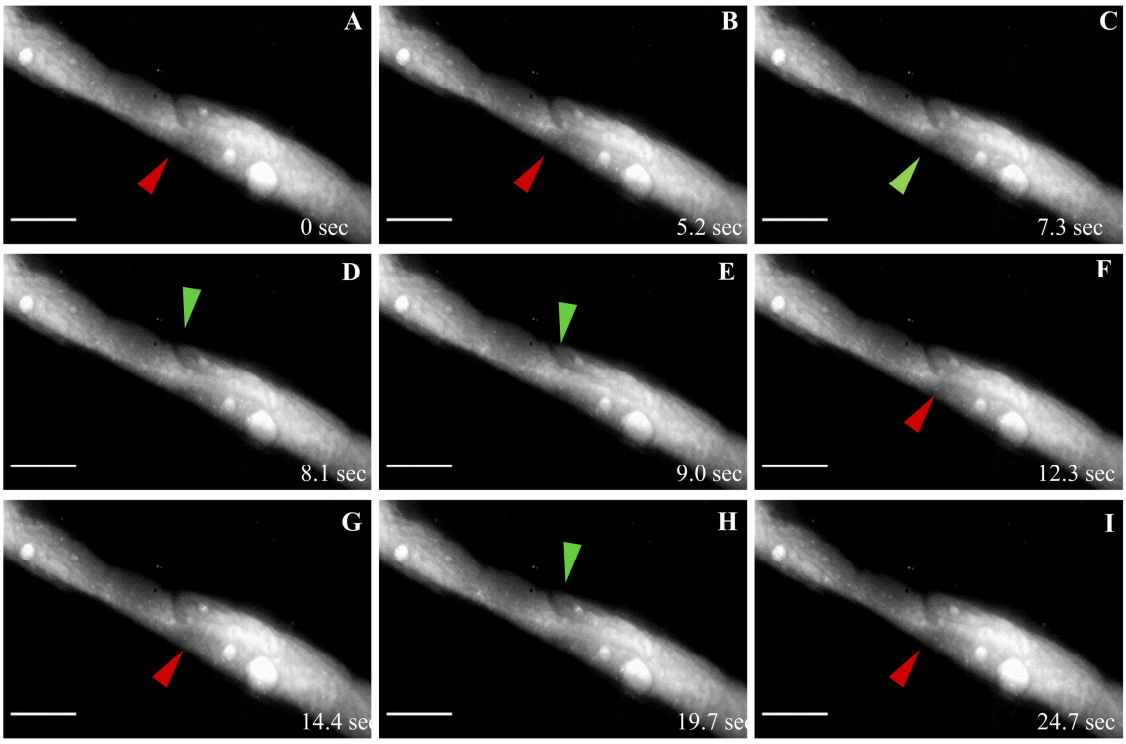

Figure 4.14. Intraluminal valve in a linear FITC-stained lymphatic vessel. The top left tract with respect to the valve is an active vessel, instead the bottom right tract is a passive segment. The valve is represented in closed (red arrowheads in panels **A-B** and **F-G-I**) or open (green arrowheads in panels **C-D** and **E-H**) state. In the bottom left corner is shown the time elapsed from the recording beginning. Scale bar: 100 µm.

Moreover, we have also been able to follow the valve dynamics during its movements, measuring a mean time from fully open to fully closed of 1.42 ± 0.19 sec (n=8).

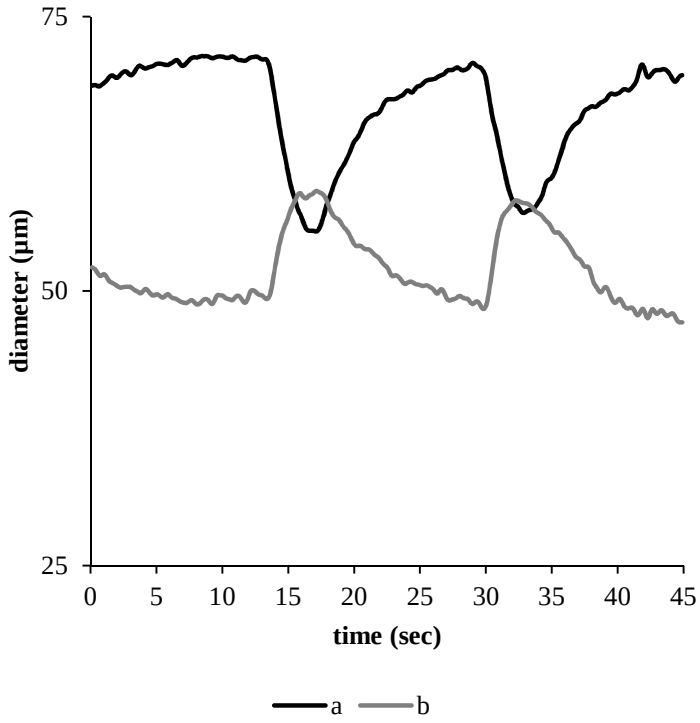

Figure 4.15. Different lymphatics behavior based on the simultaneously measured diameter changes vs time profiles. a. Pumping site in which active spontaneous contractions were found. **b**. Passive compliant site.

Through the TRITC-dextran 2% micro-injection inside the lymphatic vessel, it has been possible to demonstrate the effective presence of the valves and the net direction of lymph flow. The progression of the injected fluorescent dye bolus into a vessel was sometimes impeded by a closed valve which obstructed the lumen causing the accumulation of TRITC-dextran. When the valve was opened, it allowed fluid progression into the downstream vessel segment. In figure 4.16 it is clear that the lymph moves versus the downstream side, in effect the dye goes only in this direction.

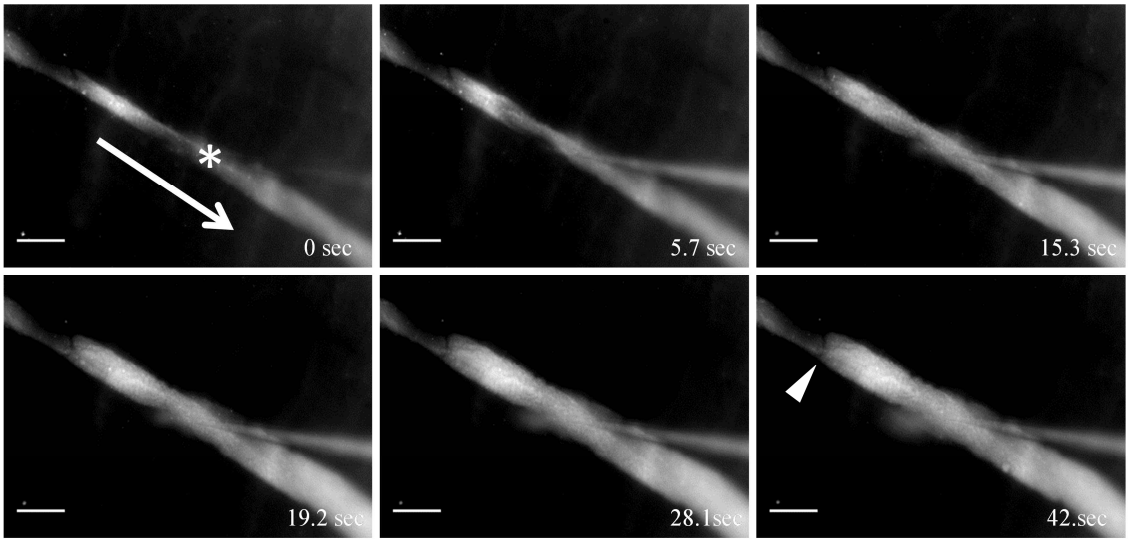

Figure 4.16. Image sequence acquired after the fluorescence injection in a lymphatic vessel. In the bottom left corner is shown the time elapsed from the recording beginning. TRITC-dextran was injected in the central side of the vessel, indicated by asterisk. The dye is progressed in the downstream region confirming the lymph flow direction (white arrow). Dye passage was obstructed by a closed valve (white arrowhead). Scale bar: 150 μm.

4.8 Epinephrine modulation

We next wanted to investigate the possible modulation exerted by epinephrine in diaphragmatic lymphatics. It is worth noting that the lymphatic collectors possess smooth muscle elements in their vessel walls. The distribution of the smooth muscle fibers surrounding lymphatic vessels are not homogenous. In contracting sites, smooth muscle elements are organized in dense meshes; conversely, in not pumping sites, smooth muscle elements are also present but they are sparsely organized (Moriondo et al., 2013).

In the first analysis, exploring in great detail the contractions of the lymphatic vessels, we have noticed different mode of contraction. Figure 4.17 proves, in a lymphatic vessel with an intraluminal valve, a particular biphasic behavior (black arrowhead and

grey arrow) obtained after epinephrine 20 μm administration, probably due to the sudden increase of contraction frequency. In the control trace (upper panel), recorded just before epinephrine administration, the biphasic mode of contraction is not present.

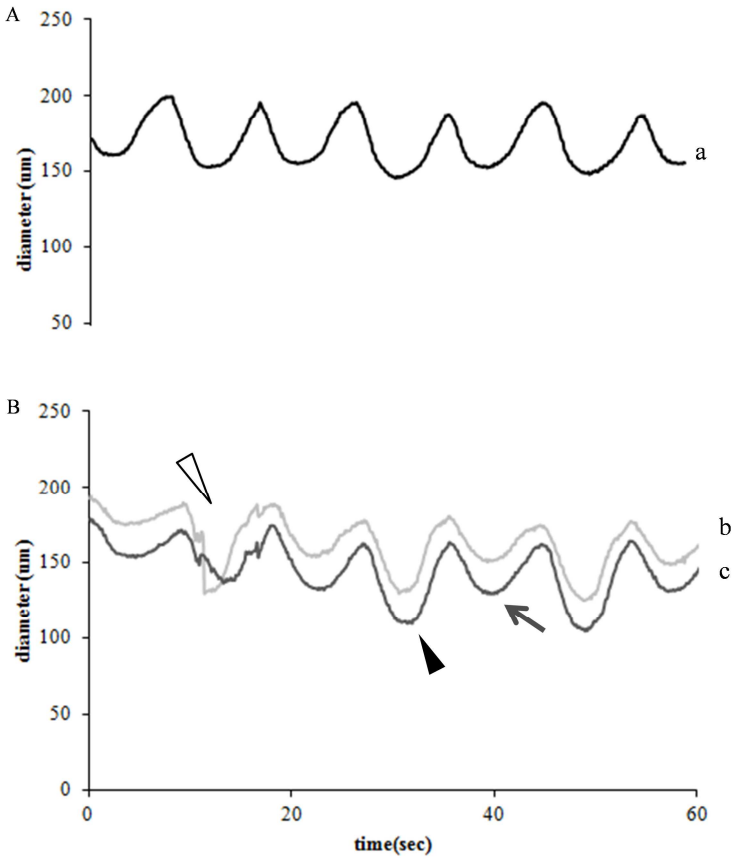

Figure 4.17. Diameter vs time profile obtained after epinephrine perfusion. **B**. The white arrow represents the moment of epinephrine administration. Biphasic contractions are evident (indicated by black arrowhead and grey arrow), both in the tract bottom right (trace **b**) than in the tract top left with respect to the valve (trace **c**). They aren't present in the monophasic control (trace **a**, panel **A**).

In effect, we were able to demonstrate that epinephrine in the diaphragmatic lymphatic loops increases the frequency of lymphatic contraction. We wanted to examine the epinephrine effect on spontaneous contractility and microsphere displacement in loop and in linear diaphragmatic lymphatics.

The results show a different behavior between loop and linear lymphatic vessels. The diameter changes of peripheral diaphragmatic loop in figure 4.18 (A) correspond exactly to microsphere progression: it is pushed forward because of the vessel contraction (C). Administration of epinephrine 20 μm, that normally acts on the smooth muscle of the vessel wall, in reality caused an increase in the contraction frequency and a decrease in stroke amplitude defined as difference between diastolic and systolic diameters (B) resulting in a greater distance traveled by the microspheres along the loop for each contraction. The mean contraction frequency due to epinephrine is higher (6.56 ± 1.62 bpm, n=4) than the loop control (3.17 ± 1.83 bpm, n=4, $p<0.01$ paired t-test) thus it is extremely significant (Figure 4.19). We interestingly found that the contraction frequency, regardless of the initial value, is always increased by epinephrine by about 3 bpm.

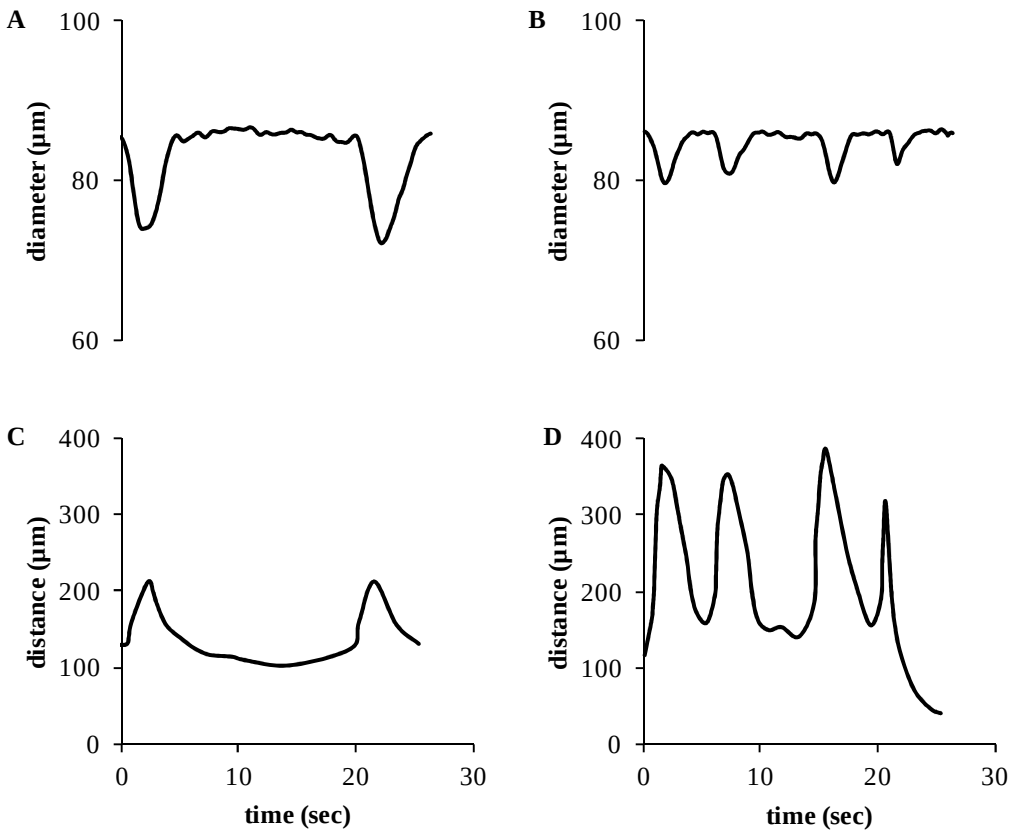

Fig. 4.18. Effect of epinephrine on spontaneous contractility and microsphere displacement in lymphatic loops. **A.** Changes over time of the diameter of lymphatic vessels in a peripheral diaphragmatic **loop**, showing active contractions. **B.** Epinephrine determined an increase in the contraction frequency and a decrease in stroke amplitude. **C**. Microsphere displacements are in phase with spontaneous vessel contractions**. D.** The greater distance traveled by the microspheres suggests a simultaneous contraction of the downstream vessel segments. Therefore, in adjacent vessel segments, epinephrine might exert either a phasic and/or a tonic effect. Zero is the distance from the contracting site.

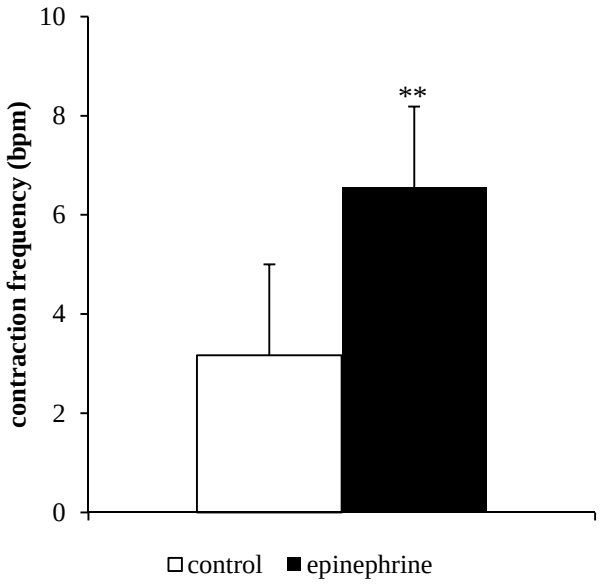

Fig. 4.19. Epinephrine effect on lymphatic loops. Mean change in contraction frequency due to epinephrine 20 μM administration in lymphatic loops. (** $p<0.01$)

Also, when the lymphatic loop did not present any contraction in control conditions, after epinephrine perfusion (Figure 4.20 - black trace) it displays active contractions.

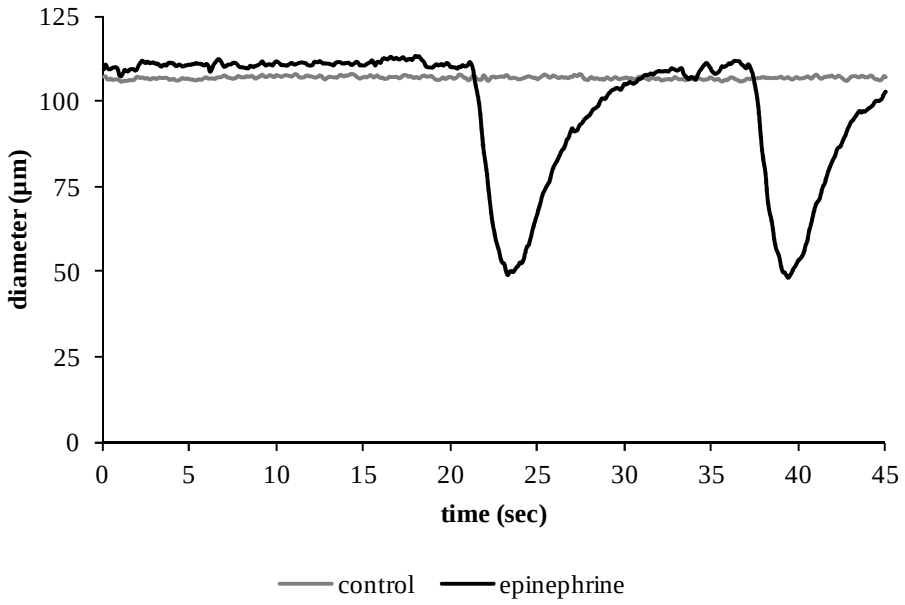

Fig. 4.20. Epinephrine effect on an invariant lymphatic loop. Changes over time of the diameter of lymphatic vessels in a peripheral diaphragmatic **loop**, that showed no active contractions (grey line). The contractions (black line) have been due to epinephrine 20 μM administration.

The figure 4.21 confirms not only that epinephrine increases the contraction frequency but also shows the effect, on the microspheres, due to the distance from contracting site even with epinephrine perfusion. When the lymphatic vessel contracts, the microsphere **a,** more distant from the contracting site (zero distance), has undergone a shorter thrust, instead the microsphere **b**, nearest to site of contraction, has undergone a major thrust.

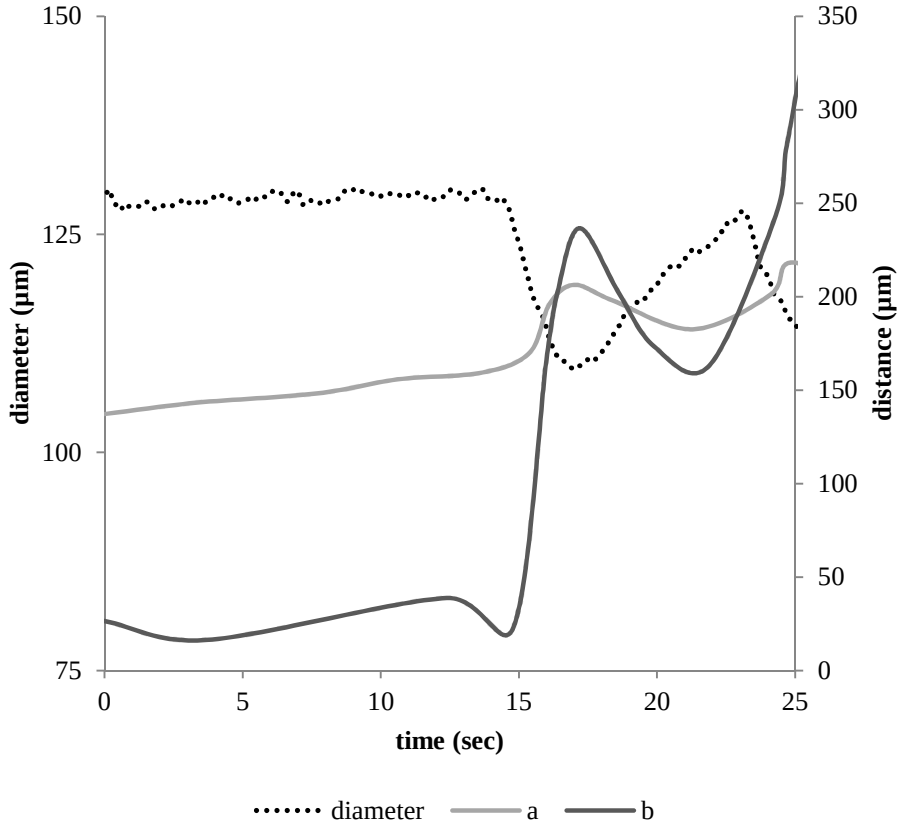

Fig. 4.21. Diaphragmatic lymphatics diameter changes and microsphere progression. Changes over time of the diameter of the diaphragmatic lymphatic vessel after epinephrine perfusion (black dotted line). Progression of closest microsphere to the contracting site (trace **a**). Progression of more distant microsphere from the contracting site (trace **b**). Zero distance represents the site of contraction**.**

The linear lymphatic vessels present however, a different behavior: considering a vessel that is spontaneously contracting (figure 4.22 A), the microsphere is displaced away from its initial site at every contraction (C); the addition of epinephrine 20 µm would

seem to block the active contraction (B) and the microspheres oscillates in a not coordinated manner (D).

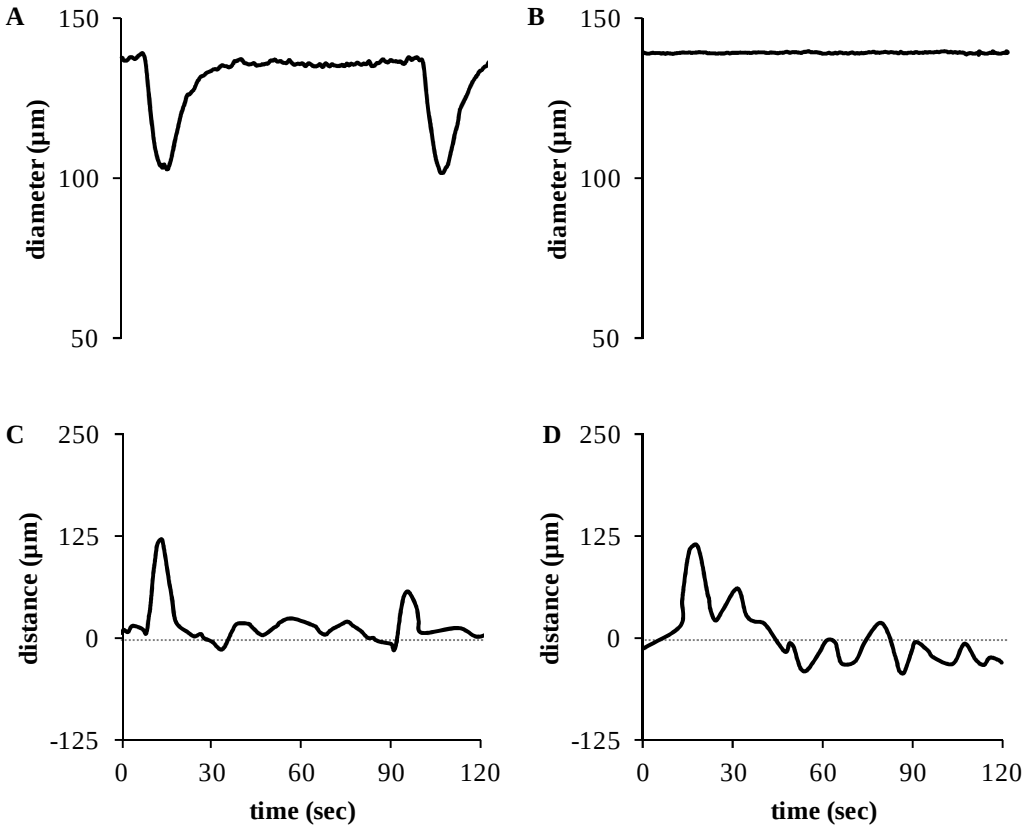

Figure 4.22. Effect of epinephrine on spontaneous contractility and microsphere displacement in linear lymphatics A. Changes over time of the diameter of a peripheral linear diaphragmatic lymphatic vessel displaying active contractions. **B.** Following 20 µm epinephrine administration lymphatic pumping activity was blocked, as indicated by the complete disappearance of vessel constriction. **C.** Displacement of a microsphere in close proximity from the contracting site. The microsphere is displaced away from its initial site at every active contraction, thereby returning towards its starting site **D.** With epinephrine, the microsphere slightly oscillates in a not coordinated manner.

The different behavior is probably due to differences of receptors in the various tracts of the vessel. The determination of the characteristics of the contractile propagation along the lymphatic network provides important information on the role of the pacemaker in the coordination of the pumping activity. The local diaphragmatic skeletal muscle contraction may modulate linear lymphatic function by compressing and expanding segmental vessel diameter and/or length. Further analysis will be conducted to demonstrate such hypothesis.

5. *Conclusions*

5. Conclusions

In diaphragmatic lymphatic vessels, spontaneous active strokes exert a distance-dependent effect on microspheres progression from the contracting site. The velocity of microspheres, that mimes the lymph progression, shows a parabolic profile within the diaphragmatic lymphatic vessels lumen.

In the presence of intraluminal valves, both in active segments and between an active and a passive tract, the microspheres show an oscillatory trajectory upstream the valve and monotonic outward directed trajectory downstream.

The Epinephrine determines:

- increase in contraction frequency and propulsive effect in *loops*;
- impairment of spontaneous activity in *linear* vessels.

Understanding the regulatory mechanisms that modulate the lymphatic functions and the lymph flow and studying molecules that regulate lymphatic muscle contraction could provide the basis for a better knowledge of the physiopathology of the lymphatic system and for the developing of innovative therapeutic strategies in order to increment the lymphatic function in pathologies due to impaired lymphatic drainage.

6. *References*

6. References

Abu-Hijleh MF, Habbal OA, Moqattash ST. The role of the diaphragm in lymphatic absorption from the peritoneal cavity. *J Anat.* **186**: 453-67, 1995

Abu-Hijleh MF and Scothorne RJ. Regional lymph drainage routes from the diaphragm in the rat. *Clinical Anatomy.* **7**: 181 – 188, 2005

Akopian VA, Balashov NV, Khanipov GF. Effect of calcitonin gene-related peptide on lymphatic vessels]. *Zh Evol Biokhim Fiziol.* **34**: 675-82, 1998

Albertine KH, Schultz EL, Wiener-Kronish JP, Staub NC. Regional differences in pleural lymphatic albumin concentration in sheep. *Am J Physiol*. **252**: H64-70, 1987

Albertine KH, Fox LM, O' Morchoe CC. The morphology of canine lymphatic valves. *Anat Rec*. **202**: 453-61, 1982

Alessandrini C, Gerli R, Sacchi G, Ibba L, Pucci AM, Fruschelli C. Cholinergic and adrenergic innervation of mesenterial lymph vessels in guinea pig. *Lymphology.* 14: 1-6, 1981

Allen EV. Lymphedema of the extremities. Classification, etiology and differential diagnosis. A study of 300 cases. *Arch Intern Med.* **54**: 602-29, 1934

Allen JM, McHale NG, Rooney BM. Effect of norepinephrine on contractility of isolated mesenteric lymphatics. *Am. J. Physiol*. **244**: H479-H486, 1983

Alitalo K, Carmeliet P. Molecular mechanisms of lymphangiogenesis in health and disease. *Cancer Cell.* **1**: 219-27, 2002

Allen WJ, Barcroft H, Edholm OG. On the action of adrenaline on the blood vessels in human skeletal muscle. *J Physiol.* **105**: 255-67, 1946

Allen JM and Bridges JB. Some effects of noradrenaline on electrical activity of guinea-pig ureteric smooth muscle. *J Med Sci.***152**: 339-48, 1983

Allen L. Lymphatics and lymphoid tissues. *Annu Rev Physiol.* **29**: 197-224, 1997

Andriotis A, Zifan A, Gavaises M, Liatsis P, Pantos I, Theodorakakos A, Efstathopoulos EP, Katritsis D. A new method of three-dimensional coronary artery reconstruction from X-ray angiography: validation against a virtual phantom and multislice computed tomography. *Catheter Cardiovasc Interv.* **71**: 28-43, 2008

Armstrong JK, Wenby RB, Meiselman HJ, Fisher TC. The hydrodynamic radii of macromolecules and their effect on red blood cell aggregation. *Biophys J.* **87**: 4259-70, 2004

Asellius G. *De lactibus sive lacteis venis.* Mediolani, Milan, 1627

Atchison DJ and Johnston MG. Role of extra- and intracellular Ca^{2+} in the lymphatic myogenic response. *Am J Physiol.* **272**: R326-33, 1997

Baluk P, Fuxe J, Hashizume H, Romano T, Lashnits E, Butz S, Vestweber D, Corada M, Molendini C, Dejana E, McDonald DM. Functionally specialized junctions between endothelial cells of lymphatic vessels. *J Exp Med.* **204**: 2349-62, 2007

Benoit JN. Effects of alpha-adrenergic stimuli on mesenteric collecting lymphatics in the rat. *Am J Physiol.* **273**: R331-6, 1997

Bény JL and Pacicca C. Bidirectional electrical communication between smooth muscle and endothelial cells in the pig coronary artery. *Am J Physiol.* **266**: H1465-72, 1994

Bettendorf U. Lymph flow mechanism of the subperitoneal diaphragmatic lymphatics. *Lymphology*. **11**: 111-116. 1978

Bettendorf U. Peritoneal resorption via lymph of diaphragm. Physiology and physiopathology. *Dtsch Med Wochenschr*. **104**: 1143-5, 1979

Beux F, Carmassi S, Salvetti MV, Ghiadoni L, Huang Y, Taddei S, Salvetti A. Automatic evaluation of arterial diameter variation from vascular echographic images. *Ultrasound Med Biol.* **27**: 1621-9, 2001

Boriek AM, Hwang W, Trinh L, Rodarte JR. Shape and tension distribution of the active canine diaphragm. *Am J Physiol Regul Integr Comp Physiol.* **288**: R1021-7, 2005

Brice G, Child AH, Evans A, Bell R, Mansour S, Burnand K, Sarfarazi M, Jeffery S, Mortimer P. Milroy disease and the VEGFR-3 mutation phenotype. *J Med Genet.* **42**: 98-102, 2005

Burgeson RE, Lunstrum GP, Rokosova B, Rimberg CS, Rosenbaum LM, Keene DR. The structure and function of type VII collagen. *Ann N Y Acad Sci.* **580**: 32-43, 1990

Casley-Smith JJR. Endothelial permeability. The passage of particles into and out of diaphragmatic lymphatics. *Q J Exp Physiol Cogn Med Sci.* **49**: 365-83, 1964

Casley-Smith JR. How the lymphatic system works. *Lymphology.* **1**: 77-80, 1968

Castenholz A. Morphological characteristics of initial lymphatics in the tongue as shown by scanning electron microscopy. *Scanning Electron Microscopy* **1984**: 1343-1352, 1984

Chen M, Marinkovich MP, Veis A, Cai X, Rao CN, O'Toole EA, Woodley DT. Interactions of the amino-terminal non collagenous (NC1) domain of type VII collagen with extracellular matrix components. A potential role in epidermal-dermal adherence in human skin. *J Biol Chem.* **272**: 14516-22, 1997

Choi I, Lee S, Hong YK. The new era of the lymphatic system: no longer secondary to the blood vascular system. *Cold Spring Harb Perspect Med.* **2**: 0-23, 2012

Cromer WE, Zawieja SD, Tharakan B, Childs EW, Newell MK, Zawieja DC. The effects of inflammatory cytokines on lymphatic endothelial barrier function. *Angiogenesis*, 2013

Dejana E, Orsenigo F, Molendini C, Baluk P, McDonald DM. Organization and signaling of endothelial cell-to-cell junctions in various regions of the blood and lymphatic vascular trees. *Cell Tissue Res.* **335**: 17-25, 2009

De Micheli P, Glässer AH. The effects of catecholamines and adrenoceptor blocking drugs on the canine peripheral lymph flow. *Br J Pharmacol.* **53**: 499-504, 1975

Dobbins DE, Swindall BT, Haddy FJ, Dabney JM. Blockade of histamine-mediated increases in microvascular permeability by H1- and H2-receptor antagonists. *Microvasc Res*. **21**: 343-50, 1981

Dobbins DE and Premen AJ. Receptor mechanisms of bradykinin-mediated activation of prenodal lymphatic smooth muscle. *Regul Pept*. **74**: 47-51, 1998

Doemling DB and Steggerda FR. Stimulation of thoracic duct lymph flow by epinephrine and norepinephrine. *Proc Soc Exp Biol Med.* **110**: 811-3, 1962

Dreyer G, Dreyer P. Rational for morbidity management in bancroftian filariasis endemic areas. *Rev Soc Bras Med Trop.* **33**: 217-21, 2000

Edery H. and Lewis GP. Kinin-forming activity and histamine in lymph after tissue injury. *J Physiol.* **169**: 568-83, 1963

Fabrice Cordelières, Manual tracking plugin. Institut Curie, Orsay (France) (fabrice.cordelieres@curie.u-psud.fr)

Ferguson MK, Shahinian HK, Michelassi F. Lymphatic smooth muscle responses to leukotrienes, histamine and platelet activating factor. *J Surg Res*. **44**: 172-7, 1988

Ferguson MK, Williams UE, Leff AR, Mitchell RW. Heterogeneity of tracheobronchial lymphatic smooth muscle responses to histamine and 5-hydroxytryptamine. *Lymphology.* **26**: 113-9, 1993

Finegold DN, Kimak MA, Lawrence EC, Levinson KL, Cherniske EM, Pober BR, Dunlap JW, Ferrell RE. Truncating mutations in FOXC2 cause multiple lymphedema syndromes. *Hum Mol Genet.* **10**: 1185-9, 2001

Fischer MJ, Uchida S, Messlinger K, Measurement of meningeal blood vessel diameter in vivo with a plug-in for ImageJ. *Microvasc Res.* **80**: 258-66, 2010

Florey HW. Observations on the contractility of lacteals. Part II. *J. Physiol*. (London) **63**: 1-18, 1927

Földi M and Zoltán OT. The effects of norepinephrine and angiotensine on the lymphatic system. *Med Pharmacol Exp Int J Exp Med*. **15**: 59-67, 1966

Foy WL, Allen JM, McKillop JM, Goldsmith JP, Johnston CF, Buchanan KD. Substance P and gastrin releasing peptide in bovine mesenteric lymphatic vessels: chemical characterization and action. *Peptides.* **10**: 533-7, 1989

Fujii J, Wernze H. Effect of vasopressor substances on the thoracic duct lymph flow. *Nature.* **210**: 956-7, 1966.

Fukuo Y, Shinohara H, Matsuda T. The distribution of lymphatic stomata in the diaphragm of the golden hamster. *J Anat.* **169**: 13-21, 1990

Galie P, Spilker RL A two-dimensional computational model of lymph transport across primary lymphatic valves. *J Biomech Eng.* 131: 111004, 2009

Gashev AA, Zawieja DC. Physiology of human lymphatic contractility: a historical perspective. *Lymphology* **34**: 124-34, 2001

Gnepp DR. The bicuspid nature of the valves of the peripheral collecting lymphatic vessels of the dog. *Lymphology*. **9**: 75-7, 1976

Gnepp DR. Lymphatics. *Edema*. Raven Press, New York, NY, pp 263-298, 1984

Gray H, Anatomy of the human body, *The lymphatic system,* 20th ed. Philadelphia: Lea and Febiger, 1918 (http://www.bartleby.com/107/175.html)

Granger DN, Mortillaro NA, Taylor AE. Interactions of intestinal lymph flow and secretion. *Am J Physiol.* **232**: E13-8, 1977

Granger H. Role of the interstitial matrix and lymphatic pump in regulation of transcapillary fluid bilance. *Microvasc Res.* **18**: 209-216, 1979

Granger H, Laine G, Barnes G & Lewis R. Dynamics and control of transmicrovascular fluid exchange. *Edema,* ed. Staub N. and Taylor A, pp.189–228. Raven Press, New York, 1984

Grimaldi A, Moriondo A, Sciacca L, Guidali ML, Tettamanti G. Negrini D. Functional arrangement of rat diaphragmatic initial lymphatic network. *Am J Physiol Heart Circ Physiol* **291**: H876-H885, 2006

Guarna M, Pucci AM, Alessandrini C, Volpi N, Fruschelli M, D'Antona D, Fruschelli C. Peptidergic innervation of mesenteric lymphatics in guinea pigs: an immunocytochemical and pharmacological study. *Lymphology.* **24**: 161-7, 1991

Haddy FJ, Scott JB, Grega GJ. Effects of histamine on lymph protein concentration and flow in the dog forelimb. *Am J Physiol.* **223**: 1172-7, 1972

Hall JG, Morris B, Woolley G. Intrinsic rhythmic propulsion of lymph in the anaesthetized sheep. *J Physiol.* 180: 336-49, 1965

Halpern W, Kelley M. In vitro methodology for resistance arteries. *Blood Vessels.* **28**: 245-51, 1991

Hammersen F. and Hammersen E. Some structural and functional aspects of endothelial cells. *Basic Res Cardiol.* **80**: 491-501, 1985

Hanley CA, Elias RM, Johnston MG. Is endothelium necessary for transmural pressure-induced contractions of bovine truncal lymphatics? *Microvasc Res.* **43**: 134-46, 1992

Hashimoto S, Inoue T, Koyama T. Serotonin reuptake inhibitors reduce conditioned fear stress-induced freezing behavior in rats. *Psychopharmacology* **123**: 182-6, 1996

Hogan RD. and Unthank JL. Mechanical control of initial lymphatic contractile behavior in bat's wing. *Am J Physiol.* **251**: H357-63, 1986

Hoogeveen RM, Bakker CJ, Viergever MA. MR phase-contrast flow measurement with limited spatial resolution in small vessels: value of model-based image analysis. *Magn Reson Med*. **41**: 520-8, 1999

Hollywood MA. and McHale NG. Mediation of excitatory neurotransmission by the release of ATP and noradrenaline in sheep mesenteric lymphatic vessels. *J Physiol.* **481**: 415-423, 1994

Hunter W. Medical Commentaries. Part I. *A. Hamilton*, London, 1762

Intaglietta M, Tompkins WR. On-line measurement of microvascular dimensions by television microscopy. *J Appl Physiol.* **32**: 546-51, 1972

Jetsch M, Tammela T, Alitalo K. and Wilting J. Genesis and pathogenesis of lymphatic vessels. *Cell Tissue Res*. **314**: 69-84, 2003

Johnston MG. and Gordon JL. Regulation of lymphatic contractility by arachidonate metabolites. *Nature.* **293**: 294-7, 1981

Johnston MG. and Feuer C. Suppression of lymphatic vessel contractility with inhibitors of arachidonic acid metabolism. *J Pharmacol Exp Ther.* **226**: 603-7, 1983

Karpanen T. and Alitalo K. Molecular biology and pathology of lymphangiogenesis. *Annu Rev Pathol.* **3**: 367-97, 2008

Lauweryns JM, Boussauw L. The ultrastructure of lymphatic valves in the adult rabbit lung. *Z Zellforsch Mikrosk Anat*. **143**: 149-68., 1973

Leak L. and Burke JF. Fine structure of the lymphatic capillary and the adjoining connective tissue area. *Am. J. Anat*. **118**: 785-810, 1966

Leak L. and Burke JF. Ultrastructural studies on the lymphatic anchoring filaments. *J. Cell. Biol*. **36**: 129-149,1968

Leak LV. and Rahil K. Permeability of the diaphragmatic mesothelium: the ultrastructural basis for "stomata". *Am. J. Anat*. **151**: 557-594. 1978

Lee J, Jirapatnakul, AC, Reeves AP, Crowe WE, Sarelius IH. Vessel diameter measurement from intravital microscopy. *Ann. Biomed. Eng.* **37**: 913–926, 2009

Lee AG, Arena CP, Beebe DJ, Palecek SP. Development of macroporous poly(ethylene glycol) hydrogel arrays within microfluidic channels. *Biomacromolecules.* **11**: 3316-3324, 2010

Lewis GP. and Winsey NJ. The action of pharmacologically active substances on the flow and composition of cat hind limb lymph. *Br J Pharmacol*. **40**: 446-60, 1970

Little TL, Xia J, Duling BR. Dye tracers define differential endothelial and smooth muscle coupling patterns within the arteriolar wall. *Circ Res.* **76**: 498-504, 1995

Marchenko SM and Sage SO. Mechanism of acetylcholine action on membrane potential of endothelium of intact rat aorta. *Am J Physiol.* **266**: H2388-95, 1994

Margaris KN and Black RA. Modelling the lymphatic system: challenges and opportunities. *J R Soc Interface.* **9**: 601-12, 2012

Mariassy AT. and Wheeldon EB. The pleura: a combined light microscopy, scanning and transmission electron microscopic study in the sheep. *Exp. Lung Res*. **4**: 293-313. 1983

Mazzoni MC, Skalak TC and Schmid-Schonbein GW. The structure of lymphatic valves in the spinotrapezius muscle pf the rat. *Blood Vessels*. **24**: 304-312, 1987

McHale NG and Roddie IC. The effect of transmural pressure on pumping activity in isolated bovine lymphatic vessels. *J Physiol.* **261**: 255-69, 1976

McHale NG and Roddie IC. Thornbury KD. Nervous modulation of spontaneous contractions in bovine mesenteric lymphatics. *J Physiol.* **309**: 461-72, 1980

McHale NG and Roddie IC. The effect of intravenous adrenaline and noradrenaline infusion of peripheral lymph flow in the sheep. *J Physiol.* **341**: 517-26, 1983

McHale NG and Allen J.M. The effect of external Ca^{2+} concentration on the contractility of bovine mesenteric lymphatics. *Microvasc. Res*. **26**: 182-192, 1983

McHale NG. Influence of autonomic nerves on lymph flow. *Lymph Stasis: Pathophysiology, Diagnosis and Treatment*, ed. Olszewski, W.L. pp. 85-107. C.R.C. Uniscience, FL, USA, 1991

McHale NG, and Meharg MK. Co-ordination of pumping in isolated bovine lymphatic vessels. *J Physiol*. **450**: 503-12, 1992

McNamee JE. Histamine decreases selectivity of sheep lung blood-lymph barrier. *J Appl Physiol Respir Environ Exerc Physiol*. **54**: 914-8, 1983

Milroy WF. An undescribed variety of herditary edema. *New York Medical Journal*, **56**: 505-508, 1892

Milroy WF. Chronic hereditary edema: Milroy's disease *Jama.* **91**: 1172-1175, 1928

Miyahara H, Kawai Y, Ohhashi T. 5-Hydroxytryptamine-2 and -4 receptors located on bovine isolated mesenteric lymphatics. *J Pharmacol Exp Ther*. **271**: 379-85, 1994

Mislin H. Active contractility of the lymphangion and coordination of lymphangion chains. *Experientia*. **32**: 820-2, 1976

Mizuno R, Koller A, Kaley G. Regulation of the vasomotor activity of lymph microvessels by nitric oxide and prostaglandins. *Am J Physiol.* **274**: R790-6, 1998

Moriondo A, Mukenge S, Negrini D. Transmural pressure in rat initial subpleural lymphatics during spontaneous or mechanical ventilation. *Am J Physiol Heart Circ Physiol.* **289**: H263-9, 2005

Moriondo A, Bianchin F, Marcozzi C, Negrini D. Kinetics of fluid flux in the rat diaphragmatic submesothelial lymphatic lacunae. *Am J Physiol Heart Circ Physiol.* **295**: H1182-H1190, 2008

Moriondo A, Solari E, Marcozzi C, Negrini D. Spontaneous activity in peripheral diaphragmatic lymphatic loops. *Am J Physiol Heart Circ Physiol.* **305**: H987-95, 2013

Negrini D, Pistolesi M., Miniati M., Bellina R., Giuntini C. and Miserocchi G. Regional protein absorption rates from the pleural cavity in dogs. *J Appl Physiol* **58**: 2062-2067, 1985

Negrini D, Mukenge S., Del Fabbro M., Gonanao C. and Miserocchi G. Distribution of diaphragmatic lymphatic stomata. *J. Appl. Physiol*. **70**: 1544-1549. 1991

Negrini D, Del Fabbro M., Gonano C., Mukenge S. and Miserocchi G. Distribution of diaphragmatic lymphatic stomata. J. Appl. Physiol. **72**: 1166-1172. 1992

Miserocchi G, Venturoli D, Negrini D, Del Fabbro M. Model of pleural fluid turnover. *J Appl Physiol* **75**: 1798-806, 1993

Negrini D, del Fabbro M, Venturoli D. Fluid exchanges across the parietal peritoneal and pleural mesothelia. *J Appl Physiol.* **74**: 1779-84, 1993

Negrini D, Ballard ST, Benoit JN. Contribution of lymphatic myogenic activity and respiratory movements to pleural lymph flow. *J Appl Physiol.* **76**: 2267-74, 1994

Negrini D, Del Fabbro M. Subatmospheric pressure in the rabbit pleural lymphatic network. *J Physiol.* **520**: 761-9, 1999

Negrini D, Moriondo A. and Mukenge S. Transmural pressure during cardiogenic oscillations in rodent diaphragmatic lymphatic vessels. *Lymphat Res Biol* **2**: 69-81, 2004

Negrini D. and Moriondo A. Lymphatic anatomy and biomechanism. *J Physiol*. **589**: 2927–2934, 2011

Ohhashi T, Kawai Y, Azuma T. The response of lymphatic smooth muscles to vasoactive substances. *Pflugers Arch.* **375**: 183-8, 1978

Ohhashi T, Kobayashi S, Tsukahara S, Azuma T. Innervation of bovine mesenteric lymphatics: from the histochemical point of view. *Microvasc Res.* **24**: 377-85, 1982

Ohhashi T, Olschowka JA, Jacobowitz DM. Vasoactive intestinal peptide inhibitory innervation in bovine mesenteric lymphatics. A histochemical and pharmacological study. *Circ Res.* **53**: 535-8, 1983

Ohhashi T, Azuma T, Sakaguchi M. Active and passive mechanical characteristics of bovine mesenteric lymphatics. *Am. J. Phisiol*. **239**: H88-H95, 1980

Ohhashi T. and Takahashi N. Acetylcholine-induced release of endothelium-derived relaxing factor from lymphatic endothelial cells. *Am J Physiol.* **260**: H1172-8, 1991

Ohtani O. Structure of lymphatics in rat cecum with special reference to submucosal collecting lymphatics endowed with smooth muscle cells and valves. I. A scanning electron microscopic study. *Arch Histol Cytol*. **55**: 429-36, 1992

Ohtani Y, Ohtani O, Nakatani T. Microanatomy of the rat diaphragm: a scanning and confocal laser scanning microscopic study. *Arch Histol Cytol* **56**: 317-328, 1993

Oliver G. and Detmar M. The rediscovery of the lymphatic system: old and new insights into the development and biological function of the lymphatic vasculature. *Genes Dev.* **16**: 773-83, 2002

Plaku KJ. and von der Weid PY. Mast cell degranulation alters lymphatic contractile activity through action of histamine. *Microcirculation.* **13**: 219-27, 2006

Pullinger BD. and Florey HW. Some observations on the structure and function of lymphatics: Their behavior in local edema. *Brit. J. Exptl. Pathol.* **16**: 49, 1935

Rockson SG. Lymphedema. *Am J Med.* **110**: 288-95, 2001

Roozendaal R, Mebius RE, Kraal G. The conduit system of the lymph node. *Int Immunol*. **20**: 1483-7, 2008

Rousselle P, Keene DR, Ruggiero F, Champliaud MF, Rest M, Burgeson RE. Laminin 5 binds the NC-1 domain of type VII collagen. *J Cell Biol.* **138**: 719-28, 1997

Sabin FR. On the origin of the lymphatic system from the veins and the development of lymph hearts and thoracic duct in the pig. *Am. J. Anat*. **1**: 367-391, 1902

Sabin FR. On the development of the superficial lymphatics in the skin of pig. *Am. J. Anat*. **9**: 43-91, 1904

Sacchi G, Weber E, Aglianò M, Raffaelli N, Comparini L. The structure of superficial lymphatics in the human thigh: precollectors. *Anat Rec.* **247**: 53-62, 1997

Scallan JP. and Huxley VH. In vivo determination of collecting lymphatic vessel permeability to albumin: a role for lymphatics in exchange. *J Physiol*. **588**: 243-54, 2010

Schad H. and Brechtelsbauer H. Thoracic duct lymph flow and composition in conscious dogs and the influence of anaesthesia and passive limb movement. *Pflugers Arch.* **371**: 25-31,1977

Schad H. and Brechtelsbauer H. Thoracic duct lymph in conscious dogs at rest and during changes of physical activity. *Pflugers Arch.* **367**: 235-40, 1977

Schad H, Flowaczny H, Brechtelsbauer H. and Birkenfeld G. The significance of respiration for thoracic duct flow in relation to other driving forces of lymph flow. *Pfluegers Arch*. **378**: 121-125, 1978

Schmid-Schonbein GW. Microlymphatics and lymph flow. *Physiol Rev*. **70**: 987-1028, 1990

Schmid-Schonbein GW. The Second Valve System in Lymphatics. *Lymphatic Research and Biology*. **1**: 25-31, 2003

Seabrook TJ, Ristevski B, Rhind SG, Shek PN, Zamecnik J, Shephard RJ, Hay JB. Epinephrine causes a reduction in lymph node cell output in sheep. *Can J Physiol Pharmacol.* **79**: 246-52, 2001

Segal SS. and Bény JL. Intracellular recording and dye transfer in arterioles during blood flow control. *Am J Physiol.* **263**: H1-7, 1992

Shim WK. and Drapanas T. Effect of intraluminal hypertonic glucose on thoracic duct lymph. *Surg Forum.* **12**: 312-3, 1961

Shinohara H. Lymphatic System of the Mouse Diaphragm: Morphology and Function of the Lymphatic Sieve. *The anatomical Record*. **249**: 6-15, 1997

Shirasawa Y. and Benoit JN. Stretch-induced calcium sensitization of rat lymphatic smooth muscle. *Am J Physiol Heart Circ Physiol*. **285**: H2573-7, 2003

Shulte Merker S, Sabine A, Petrova TV. Lymphatic vascular morphogenesis in development, physiology, and disease. *J. Cell Biol.* **193**: 607-618, 2011

Simons MA, Bastian BV, Bray BE, Dedrickson DR. Comparison of observer and videodensitometric measurements of simulated coronary artery stenoses. *Invest Radiol*. **22**: 562-8, 1987

Sleeman JP. and Thiele W. Tumor metastasis and the lymphatic vasculature. *Int J Cancer*. **125**: 2747-56, 2009

Smith RO. Lymphatic contractility: a possible intrinsic mechanism of lymphatic vessels for the transport of lymph. *J Exp Med.* **90**: 497-509, 1949

Swartz MA. The physiology of the lymphatic system. *Adv Drug Deliv Rev*. **50**: 3-20, 2001

Spagnoli LG, Villaschi S, Neri L, Palmieri G. Gap junctions in myo-endothelial bridges of rabbit carotid arteries. *Experientia.* **38**: 124-5, 1982

Svensjö E, Adamski SW, Su K, Grega GJ. Quantitative physiological and morphological aspects of microvascular permeability changes induced by histamine and inhibited by terbutaline. *Acta Physiol Scand.* **116**: 265-73, 1982

Tammela T. and Alitalo K. Lymphangiogenesis: Molecular mechanisms and future promise. *Cell.* 140: 460-76, 2010

Takada M. The ultrastructure of lymphatic valves in rabbits and mice. Am *J Anat.* **132**: 207-17, 1971

Takahashi T, Kawai Y, Ohhashi T. Effects of vasoconstrictive and vasodilative agents on lymphatic smooth muscles in isolated canine thoracic ducts. *J Pharmacol Exp Ther.*. **254**: 165-170, 1990

Trzewik J, Mallipattu SR, Artmann GM, DeLano FA. and Achmid-Schonbein G.W. Evidence for a second valve system in lymphatics endothelial microvalves. *FASEB J*. **15**: 1711-1717, 2001

Tsilibary EC and Wissig SL. Absorption from the peritoneal cavity: SEM study of the mesothelium covering the peritoneal surface of the muscular portion of the diaphragm. *Am J Anat.* **149**: 127-33, 1977

Unterberg A, Wahl M, Baethmann A. Effects of bradykinin on permeability and diameter of pial vessels in vivo. *J Cereb Blood Flow Metab.* **4**: 574-85, 1984

van der Putte SC. The development of the lymphatic system in man. *Adv Anat Embryol Cell Biol.* **51**: 3-60, 1975

Van Helden DF. and Zhaoj. Lymphatic vasomotion. *Clin Exp Pharmacol Physiol*. **27**: 1014-1018, 2000

Vas R, Eigler N, Miyazono C, Pfaff JM, Resser KJ, Weiss M, Nivatpumin T, Whiting J, Forrester J. Digital quantification eliminates intraobserver and interobserver variability in the evaluation of coronary artery stenosis. *Am J Cardiol.* **56**: 718-23, 1985

von der Weid PY. and Bény JL. Simultaneous oscillations in the membrane potential of pig coronary artery endothelial and smooth muscle cells. *J Physiol.* **471**: 13-24, 1993

von der Weid PY, Crowe MJ, Van Helden DF. Endothelium-dependent modulation of pacemaking in lymphatic vessels of the guinea-pig mesentery. *J Physiol.* **493**: 563-75, 1996

von der Weid PY. and Van Helden DF. Functional electrical properties of the endothelium in lymphatic vessels of the guinea-pig mesentery. *J Physiol.* **504**: 439-51, 1997

von der Weid PY. and Zawieja DC. Lymphatic smooth muscle: the motor unit of lymph drainage. *Int J Biochem Cell Biol*. **36**: 1147-1153, 2004

Yip CY, Aggarwal SJ, Diller KR, Bovik AC. Simultaneous multiple site arteriolar vasomotion measurement using digital image analysis. *Microvasc. Res.* **41**: 73–83, 1991

Wang NS. Anatomy of the pleura. *Clin Chest Med*. **19**: 229-240

Wang NS. The preformed stomata connecting the pleural cavity and the lymphatics in the parietal pleura. *Am. Rev. Respir. Dis*. **111**: 12-20. 1975

Webb R. Behavior of lymphatic vessels in the living bat. *Anat Rec*. **88**: 351-367, 1944

Williamson IM. Some responses of bovine mesenteric arteries, veins and lymphatics. *J Physiol.* **202**: 112P, 1969

Zawieja DC, Kossman E, Pullin J. Dynamic of the microlymphatic system. *J Prog Appl Microcirc*. **23**: 100-109, 1999

Zawieja DC. Contractile physiology of lymphatics. *Lymphat Res Biol*. **7**: 87-96, 2000.

Acknowledgements

I would like to thank my family and everyone who helped me, during my PhD period at the Department of Surgical and Morphological Sciences, University of Insubria of Varese, and have become my friends.

A very special thank to Professor Daniela Negrini, who let me to work in her research group, for the precious scientific suggestions and for her support, during the development of my project.

I'm very grateful to Dr. Andrea Moriondo for his great patience, for his help and for his brilliant ideas.

I would like to thank Cristiana and Eleonora for their valuable help and for their friendship.